Polyphase-Coded FM Waveform Optimization within a LINC Transmit Architecture

By

Lane S. Ryan

Submitted to the graduate degree program in Electrical Engineering and Computer Science and the Graduate Faculty of the University of Kansas in partial fulfillment of the requirements for the degree of Master of Science.

_____

Chairperson Dr. Christopher Allen

_____

Dr. Shannon Blunt

_____

Dr. James Stiles

Date Defended: January 16th, 2014

The Thesis Committee for Lane S. Ryan

certifies that this is the approved version of the following thesis:

Polyphase-Coded FM Waveform Optimization within a LINC Transmit Architecture

_____

Chairperson Dr. Christopher Allen

Date approved:

Acknowledgements

I would like to thank Dr. Allen and Dr. Blunt for all of their ideas and support throughout this process. I would also like to give a special thanks to John Jakabosky for the many hours he spent helping me. None of this would have been possible without these three people. This work pushed our current lab equipment to its very limit and I need to thank Dan DePardo and Dr. Seguin for their help in equipping me with the necessary hardware to pull this off. Thanks also to my committee members: Dr. Allen, Dr. Blunt, and Dr. Stiles. My family deserves thanks for all their love and support. My parents, Ed and Susan Ryan, have given me every opportunity possible to be successful in life and I owe a lot to them. Finally, I give thanks to my wife, Chelsea Ryan, who has encouraged and supported this and all my pursuits since they day we met.

Abstract

Linear amplification using nonlinear components (LINC) is a design approach that can suppress the effects of the nonlinear distortion introduced by the transmitter. A typical transmitter design requirement is for the high power amplifier to be operated in saturation. The LINC approach described here employs a polyphase-coded FM (PCFM) waveform that is able to overcome this saturated amplifier distortion to greatly improve the spectral containment of the transmitted waveform. A two stage optimization process involving simulation and hardware-in-the-loop routines is used to create the final PCFM waveform code.

Contents

List of Figures

List of Tables

1 Introduction

1.1 Background

Transmitters are vital elements in a variety of microwave and RF systems – wireless communications, GPS, broadcast services, and radar systems. It is the transmitter that often dominates a system's overall power consumption, determines its maximum range, and radiated spectral content. The design decisions regarding transmitter components/topology, modulation scheme, and excitation waveform are critical to the desired performance of the system.

A significant challenge of transmitter design is the issue of spectral containment. The RF spectrum is an already crowded space, which driven by commercial communications, will only continue to get more crowded. Due to this, radar usage of the RF spectrum might soon be facing stricter regulations [1,2]. Radar Spectrum Engineering Criteria (RSEC) is a set of rules that establishes the required spectral roll-off and out-of-band limit for radiated emissions. There is an ongoing discussion to modify RSEC by increasing the required spectral roll-off from 20 dB/decade to 30 or even 40 dB/decade. Also, it is being explored to decrease the lower out-of-band limit to at least 60 dB relative to the peak power of the carrier frequency. The RF spectrum is obviously a finite resource, so stricter requirements placed on spectral containment has all the makings of inevitability. This creates some interesting challenges for the design of radar transmitters and their emissions [3].

1.2 Objectives

The primary goal of this work is to create a transmitter topology that addresses the fundamental concern of spectral containment, specifically overcoming the inherent drawbacks of transmitter power amplifiers operating in saturation. Also, a process needs to be created to take a continuous phase modulation (CPM) linear FM (LFM) chirp to an optimized non-linear FM (NLFM) waveform within this new transmitter topology. This optimization process will seek to minimize the peak sidelobes of the autocorrelation of the received radar pulse. Another goal is to make the radar system as robust as possible. Primarily, the system needs to be resilient to transmitter amplifier mismatch and timing skew effects.

1.3 Organization

This thesis is organized into 6 sections. The information contained in these chapters is listed below:

- Section 2 discusses waveform design, describes CPM, and goes over the optimization algorithm and parameters.
- Section 3 will explain the LINC configuration and the advantages/disadvantages of this approach.
- Section 4 is about the hardware implementation. Challenges encountered are discussed and earlier configurations are compared to the final hardware configuration.
- Section 5 presents and analyzes the experimental results.
- Section 6 gives conclusions, suggested improvements, and possible future work.

2 Waveform Design

2.1 Modulation

CPM is used in a variety of applications such as aeronautical telemetry and deep-space communications. It is the basis of the Bluetooth standard. Its chief advantages are power efficiency (due to constant modulus) and spectral efficiency. Power efficiency is incredibly important in radar applications because it is directly related to how much energy can be put on target. Spectral efficiency is extremely important for the reasons described in the introduction. These traits make the CPM framework a good candidate for the objectives of this effort. The PCFM waveform generation is shown in Fig. 2.1.

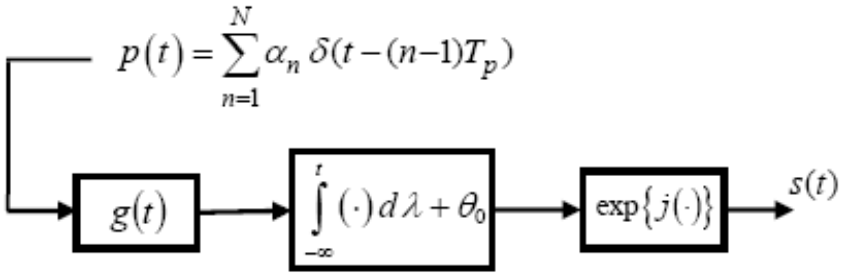

Figure 2.1. PCFM radar waveform implementation

The input, $p(t)$, is a train of N impulses with separation T_p such that the total pulsewidth is $T = NT_p$. The shaping filter g(t) can be any arbitrary shape as long as it is scaled to integrate to unity and has time support on [0, T_p]. The phase change between successive chips in the code is defined as

$$\alpha_n = \begin{cases} \tilde{c}_{\cdot\cdot} & \text{if } |\tilde{c}_{\cdot\cdot} \\ \tilde{c}_{\cdot\cdot} & \end{cases} \tag{1}$$

where

$$\tilde{c}_{\quad\quad\quad} \quad \text{for} \quad n=1,\cdots \quad , \tag{2}$$

and θ_n is the phase of the n^{th} element in a length of N+1 polyphase code. The resulting baseband output s(t) is a form of nonlinear FM (NLFM) that can be modulated onto a carrier.

2.2 Optimization

This CPM implementation allows for the optimization of discrete code values **and** the assessment of the resulting physical emission [4-6]. Figure 2.2 is a conceptual illustration of a new paradigm in code design that includes the generation of the continuous waveform via this CPM implementation.

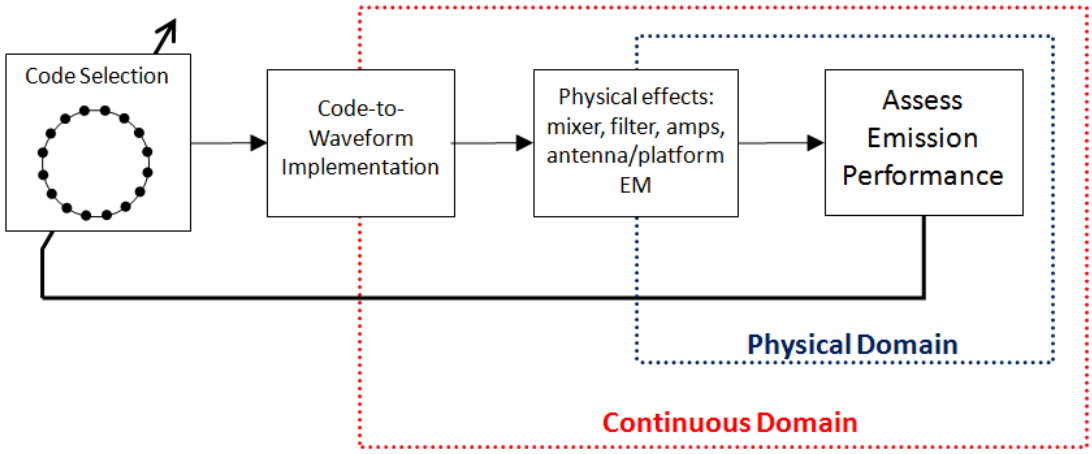

Figure 2.2. Transmitter-in-the-loop emission optimization

The physical effects imposed by the transmitter are included in this process as well so that the decision driven optimization algorithm is based on the ultimate physical emission. This holistic design approach that considers both the discrete waveform code selection and that actual physical emission is crucial to the design philosophy used in this endeavor. It should be noted, that in many publications, this philosophy was not employed. Instead, the design of RF emissions has historically focused on either maximizing power efficiency while maintaining signal quality or developing theoretical excitation waveforms that will yield better performance

(e.g.. bit-error rate, peak range sidelobe ratio, impulse response). The limitation of this type of isolated approach is that it does not account for the actual interaction between excitation waveform and transmitter. If the excitation waveform and the transmitter are considered independently, it is often not until full system integration when the detrimental effects of these neglected interactions between hardware and waveform become evident. The main source of distortion in a transmitter is typically from the power amplifier (PA). The causes and effects of this introduced distortion are gone over in detail in the following section.

The optimization scheme used here employs a greedy search strategy [4,6] that does not guarantee the global minimum but has been shown to yield quite good solutions nonetheless. The peak sidelobe level (PSL) of the received waveform's autocorrelation is the optimization parameter. The goal is to minimize the PSL. Unfortunately, the global minimum cannot be guaranteed because the PSL cost function is not convex and an exhaustive search is not feasible as the number of unique waveforms is exceedingly high. For example, for $N = 64$ phase transitions in the code and $M = 64$ possible phase states there are $M^N = 64^{64} = 3.9402 \times 10^{115}$ possible unique waveforms.

For the optimization, first a "phase change" version of the code, defined as $\mathbf{x} = [\alpha_1\ \alpha_2\ \ldots\ \alpha_N]$, is initialized with some starting phase sequence. Next, using the CPM implementation from Figure 2.1, a PCFM waveform is then generated from this code. Then α_1 is cycled through every possible phase change within a discrete sampling over $[-\pi, \pi]$, with the value generating the minimum PSL being kept. The 2nd and 3rd steps are then repeated with n = 2, 3,…, N until no single value of α_n can be changed to provide a lower PSL. This greedy approach is vitally important as it has a search space on the manageable order of MN as opposed to M^N, which was shown above to be intractable.

Since it is not an exhaustive search, the effectiveness of the hardware-in-the-loop optimization does depend on the initial code that is used to seed the search algorithm. Due to this, the optimization is performed in two stages. The first stage is simulation based and done purely in Matlab. This simulation is simply seeded with an LFM chirp (P3 code). The starting code is somewhat arbitrary because very fast optimization can be performed in the simulation environment (e.g. at present roughly 17,000 waveforms can be analyzed per second using a high-performance GPU). By comparison, for the test equipment employed in this experiment, only one waveform can be analyzed every 1.5 seconds when the transmitter hardware is included. In theory, the simulation stage is actually unnecessary but the amount of time the optimization would last on hardware might be considered unreasonably long. The simulation stage of the optimization makes this entire two stage process take a matter of hours, literally shaving days off the process. Due to the incredible time-savings, the hardware-in-the-loop optimization should be seeded with a waveform previously optimized in simulation so as to start out in the general neighborhood of a good result.

3 LINC

3.1 Overview

Linear amplification using nonlinear components (LINC) is a paradigm that is employed here by combining 2 radar waveforms in a 180° coupler and manipulating their relative phases to control the amplitude of the resulting summed waveform [7,8].

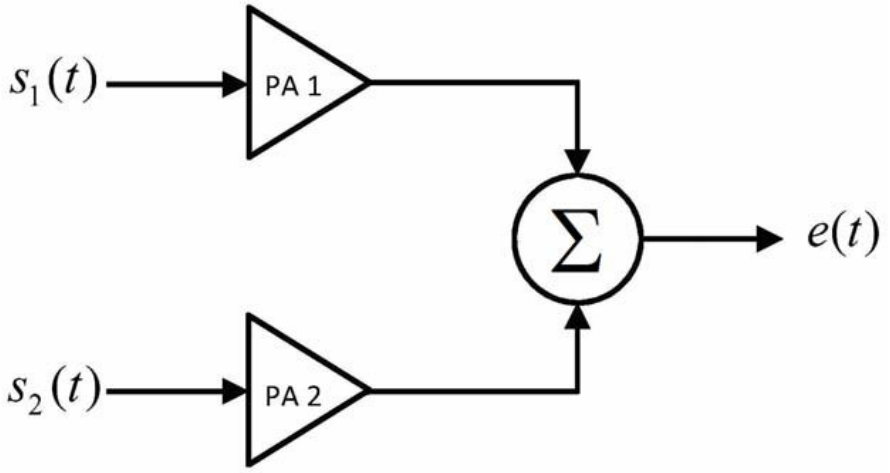

Figure 3.1. 180° coupler LINC transmitter implementation

To go into more detail, two continuous waveforms $s_1(t)$ and $s_2(t)$ are generated such that their relative phases, when combined in a 180° coupler (see Fig. 3.1), creates a phase-modulated pulse $e(t)$ whose amplitude follows some desired shape. The purpose of this is to manipulate the pulse rise/fall-time in order to control the spectral content of the pulse. By controlling the relative phases of $s_1(t)$ and $s_2(t)$, as shown in Figure 3.2, the amplitude tapering of $e(t)$ is produced (see Fig. 3.3). To generate the tapering effect, waveform $s_2(t)$ is modified with respect to waveform

$s_1(t)$ at the beginning and end of the pulse by changing the associated values of α_n for the 2nd waveform.

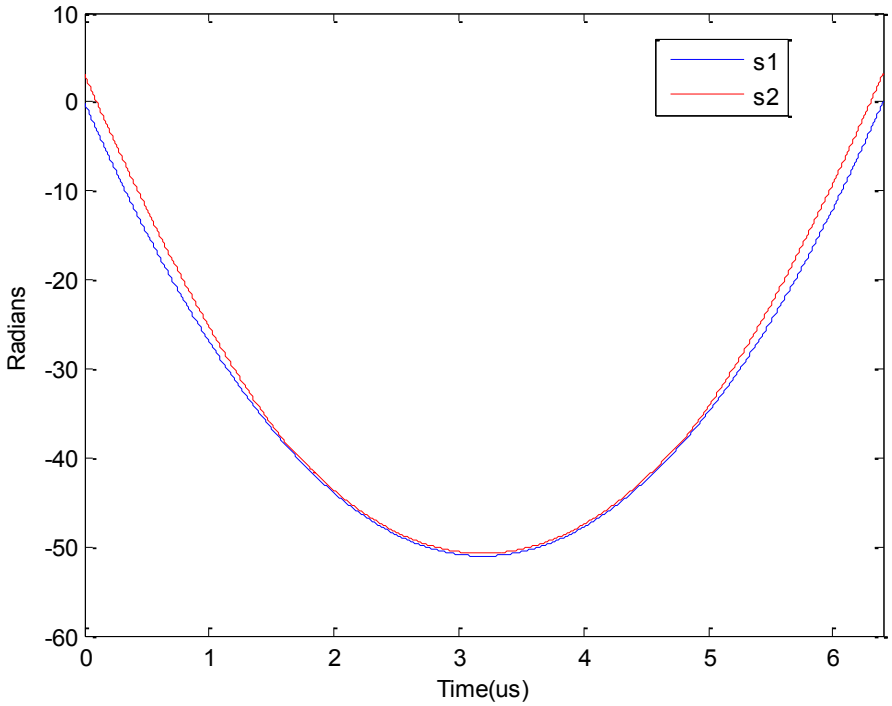

Figure 3.2. Unwrapped phase of waveforms $s_1(t)$ and $s_2(t)$

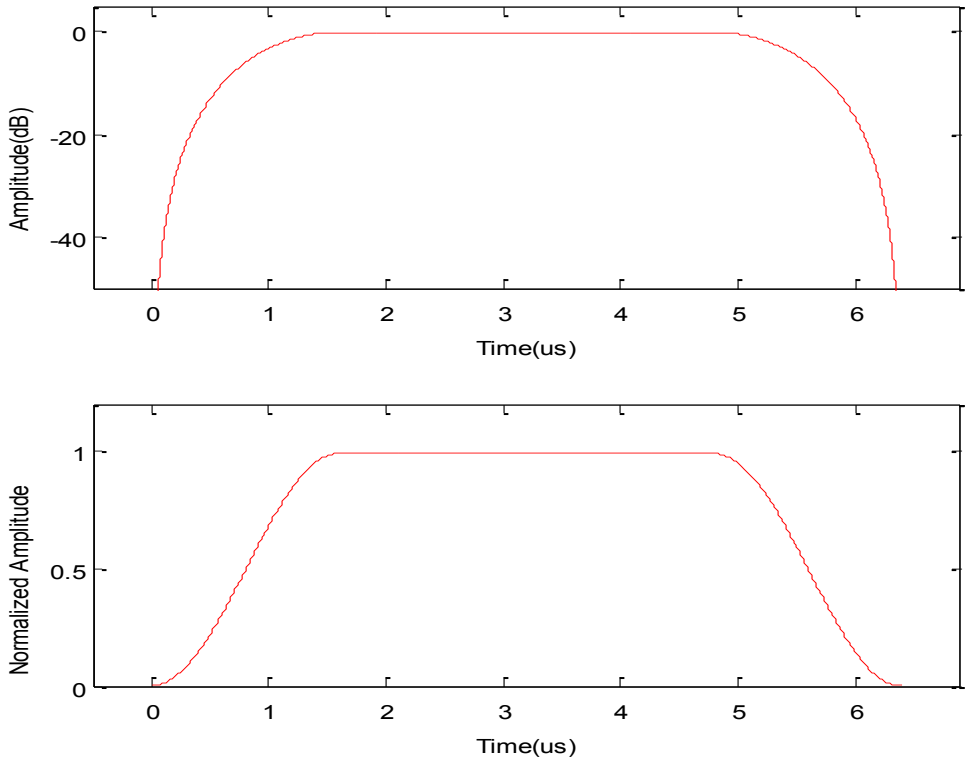

Figure 3.3. 16 chip amplitude taper Tukey window

3.2 Motivation

To maximize power efficiency and thus energy-on-target, a common radar requirement is for the transmitter power amplifier (PA) to be operated in saturation. The constant modulus and relatively bandlimited attributes of FM waveforms (such as PCFM) helps to naturally negate most of the effects of operating in the nonlinear regime of the power amplifier. However, this nonlinearity also precludes the use of an amplitude taper to increase the spectral containment of the transmitted waveform by "slowing down" the otherwise rapid rise/fall-time of the pulse. The LINC strategy addresses this issue by using two matched power amplifiers. Amplitude manipulation of the pulse can be achieved directly by changing the relative phases of the two waveforms. Since both amplifier outputs are constant amplitude, the nonlinear effects of saturation are almost completely negated.

The LINC approach is a powerful tool that allows for the creation of waveforms that could not be easily implemented with a single amplifier design. With this setup, it is possible to apply a taper to a pulse without experiencing the negative nonlinear effects of the components involved. Tapering is well known as a means to reduce range sidelobes for an LFM chirp [9]. The difficulty is that tapers are very problematic to implement with a single saturated amplifier. However, if the output amplitudes of two parallel amplifiers can be calibrated to match reasonably well, then amplitude manipulation of the resulting emission can be attained through the phasing in and out of the two input waveforms.

3.3 The Tukey Window

The Tukey window was the amplitude taper of choice used in this experimentation. It provided desirable spectral containment, is adjustable, and easily implemented within the LINC architecture. The Tukey window is defined as follows:

$$w(x) = \begin{cases} \frac{1}{2}\{1+\cos(\frac{2\pi}{r}[x - r/2])\} & 0 \le x < \frac{r}{2} \\ 1 & \frac{r}{2} \le x < 1 - \frac{r}{2} \\ \frac{1}{2}\{1+\cos(\frac{2\pi}{r}[x - 1 + r/2])\} & 1 - \frac{r}{2} \le x \le 1 \end{cases}$$

where r is the ratio of cosine-tapered section length to the entire window length. This tapering effect is obvious in Figure 3.3. As mentioned, the Tukey window is adjustable by varying r. With a very short taper length, the Tukey window will approach a rectangular window. At the other extreme, the Tukey window becomes a Hanning window, where there is no flat portion of the pulse amplitude. The trade-off is simple. A longer taper length results in better spectral containment but comes at the cost of reduced SNR. The following table shows this trade-off numerically.

Table 3.1. Tukey window SNR degradation

r	Chip length	SNR degradation
0.125	4	-0.7093
0.5	16	-3.2573
1	32	-8.5221

The chip length column represents the number of chips at the beginning and end of the pulse that the taper will be applied. Experimental results are provided later for 4 chip and 16 chip taper

length implementations. The 32 chip taper length was included for comparison purposes and represents the absolute extreme case where the Tukey window becomes a Hanning window.

To quantify this difference in terms of energy, the energy of a single pulse in the experiment setups without the taper applied is roughly 300 nJ. A 4 chip taper length will reduce that to 281.25 nJ, the 16 chip taper will reduce it even further to 225 nJ, and the 32 chip taper length will cut it in half to 150 nJ.

The specific purpose of the taper is to "slow down" the pulse rise time, but not greatly attenuate the entire pulse. The Tukey window fits this design criteria the best. There are alternatives, such as: the modified Bartlett-Hann window, Blackman window, Blackman-Harris window, Bohman window, Gaussian window, Hamming window, and Taylor window. However, some of these alternatives are not adjustable and all of these alternatives require significant attenuation of the pulse amplitude. None of these windows allow for a flat, sustained maximum amplitude (as seen in Fig. 3.3). Due to these drawbacks, the Tukey window was selected as the best established tapering method.

4 Hardware Implementation

4.1 Challenges

There were significant challenges encountered trying to implement the LINC architecture in hardware. The relative timing of the two waveforms requires nearly perfect stability for the optimization routines to work. The original configuration is shown in the following figure.

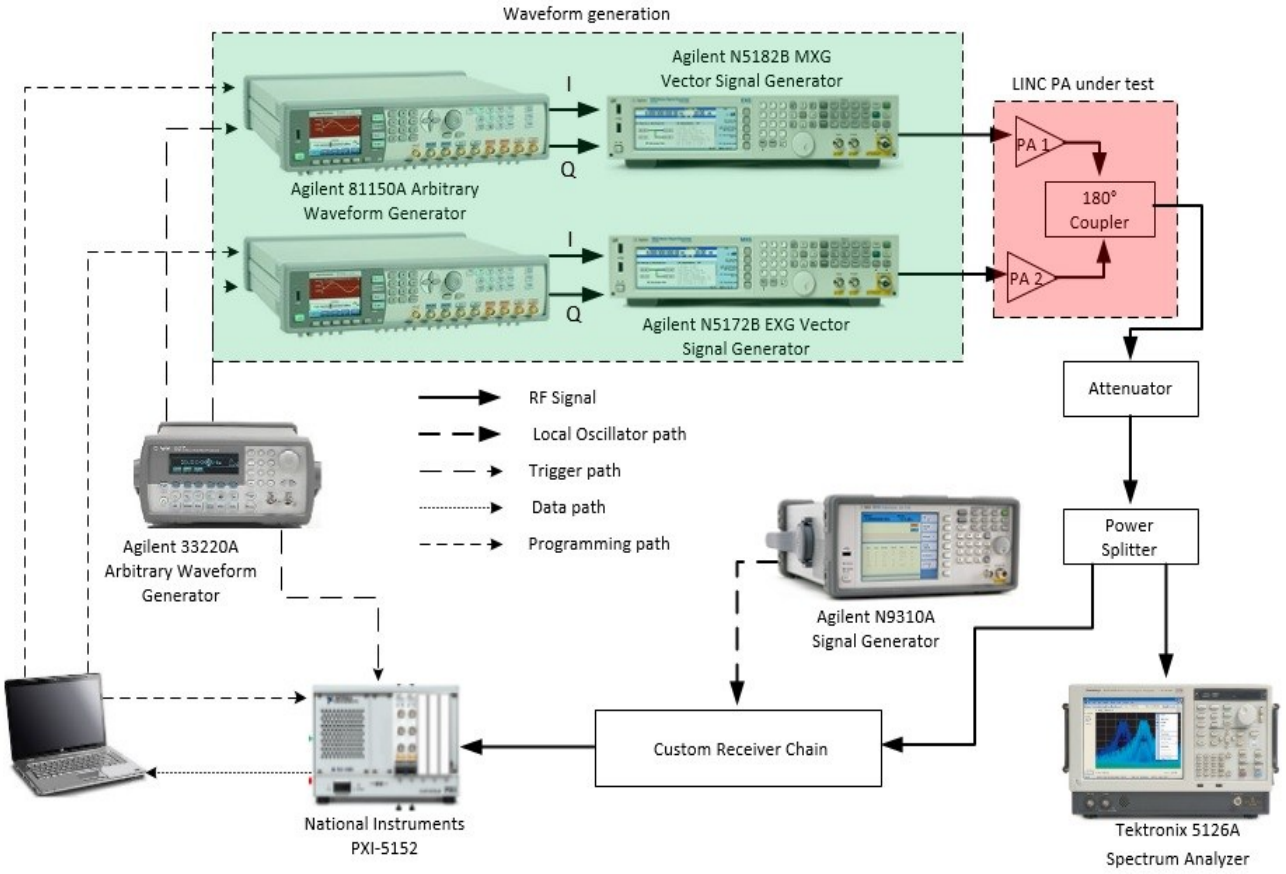

Figure 4.1. Original radar testbed configuration

Timing stability made this configuration untenable. The waveforms were generated by two identical arbitrary waveform generators, then modulated onto the carrier frequency by two signal generators. It was impossible to get the necessary timing synchronization between these 4

instruments to get a stable waveform coming out of the hybrid coupler. The LO's of the two signal generators could be adjusted to calibrate any timing skew between the two waveforms. However it was not sensitive enough to be of real use. For the LINC approach to truly work, there needs to be nearly perfect cancellation when the two waveforms are completely out-of-phase. Even when the timing was calibrated as well as possible, the relative phases of the two waveforms entering the hybrid coupler would drift. There was no way to lock the respective LO's of the two signal generators. Time consuming optimizations were not possible because the system would be changing during the optimization routine, ruining any results. The system was also very thermally sensitive. The instruments required several hours of warm up time to even be stable over the course of a few minutes.

4.2 Final Instrument Configuration

The initial configuration was eventually abandoned as unusable for this optimization process and an alternative instrument configuration was employed.

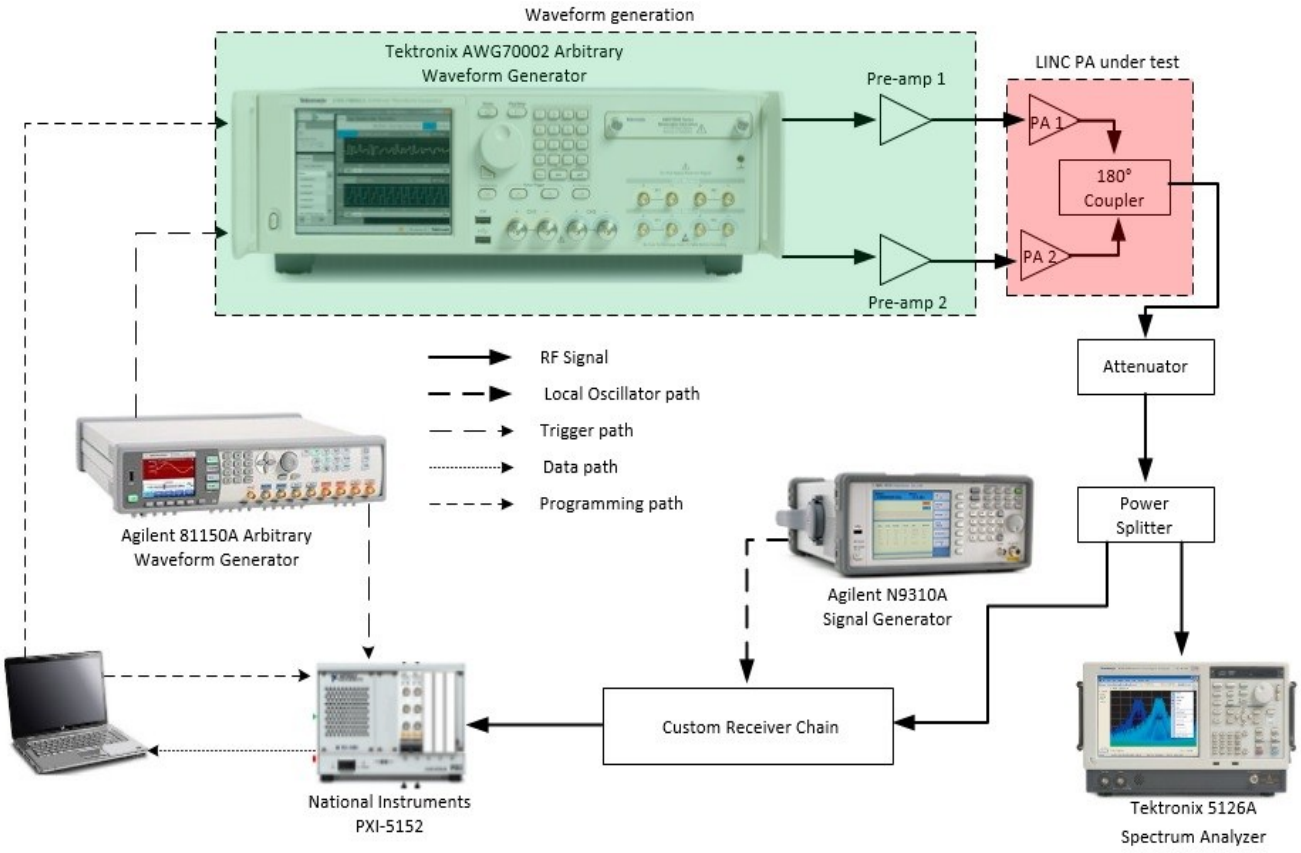

Figure 4.2. Final configuration of the radar testbed

This configuration had the advantage of having a dual channel arbitrary waveform generator with two RF outputs. This one instrument effectively replaced four instruments from the previous configuration; the green shaded area represents the differences between the two configurations. This exchange of instruments gave the necessary timing stability needed to perform the optimization routines. It had the ability to adjust the timing skew between the two RF outputs by 0.5 ps increments. This allowed for a very fine calibration of the relative phases of the two waveforms entering the hybrid coupler, an absolutely vital ability in order for the LINC strategy to function properly.

4.3 Component Configuration

Experimental results were obtained with three different transmitter configurations. The first configuration (see Fig. 5.1) uses no transmitter PA's. This represents the best case scenario with zero amplifier distortion. The other two configurations (see Fig 5.8 and 5.15) represent reasonable PA distortion and worst case PA distortion, respectively. Both of these configurations utilize a pair of first stage amplifiers that are NOT considered to be under test. Their purpose is only to put the next pair of amplifiers well into saturation. All amplifiers are characterized with a network analyzer with a center frequency of 1.8425 GHz and a span of 110 MHz. The first stage amplifiers are characterized in Figures 4.3 and 4.4. The amplifiers are identical models and output responses are acceptably similar, as expected.

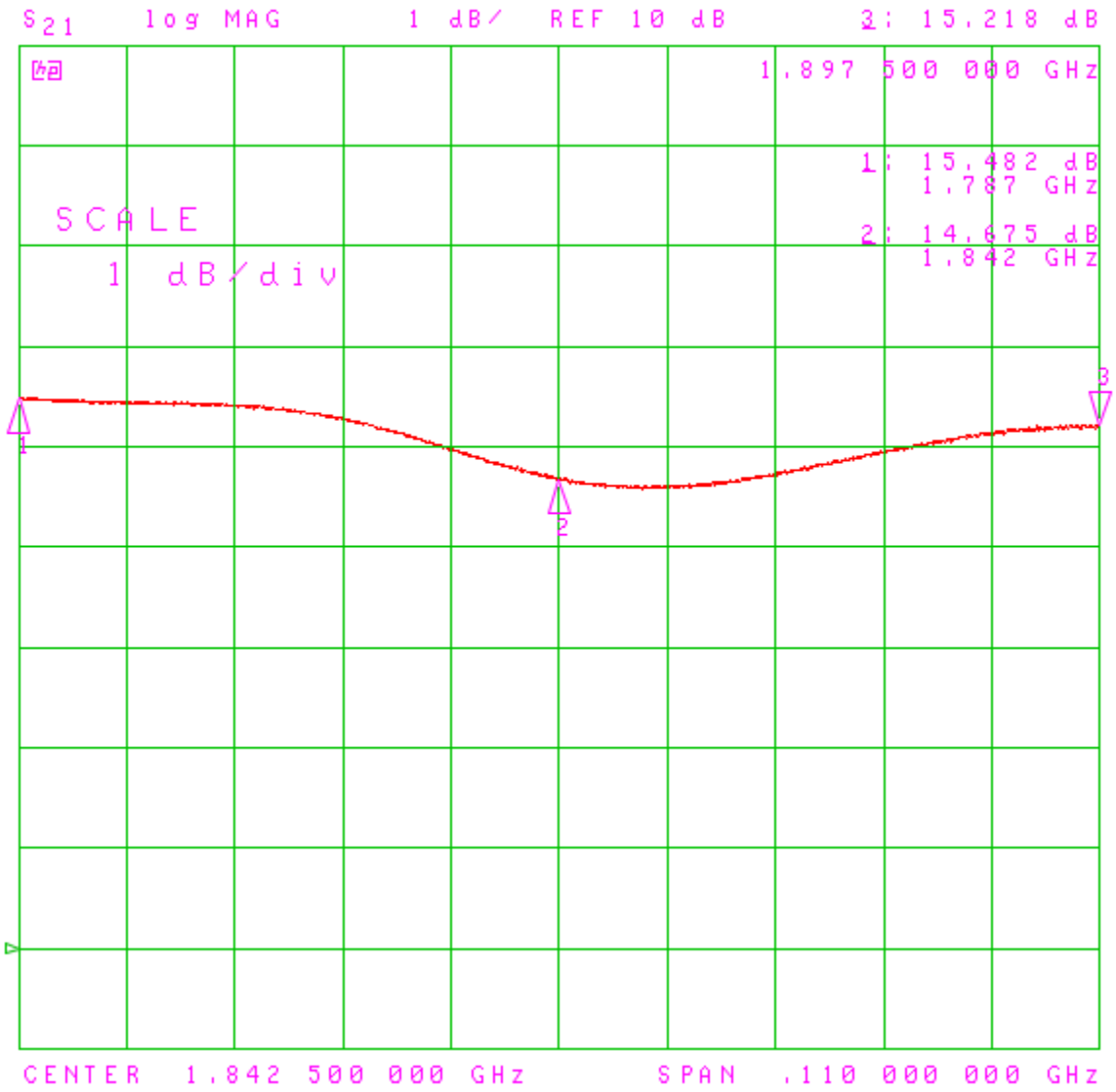

Figure 4.3. First stage amplifier 1

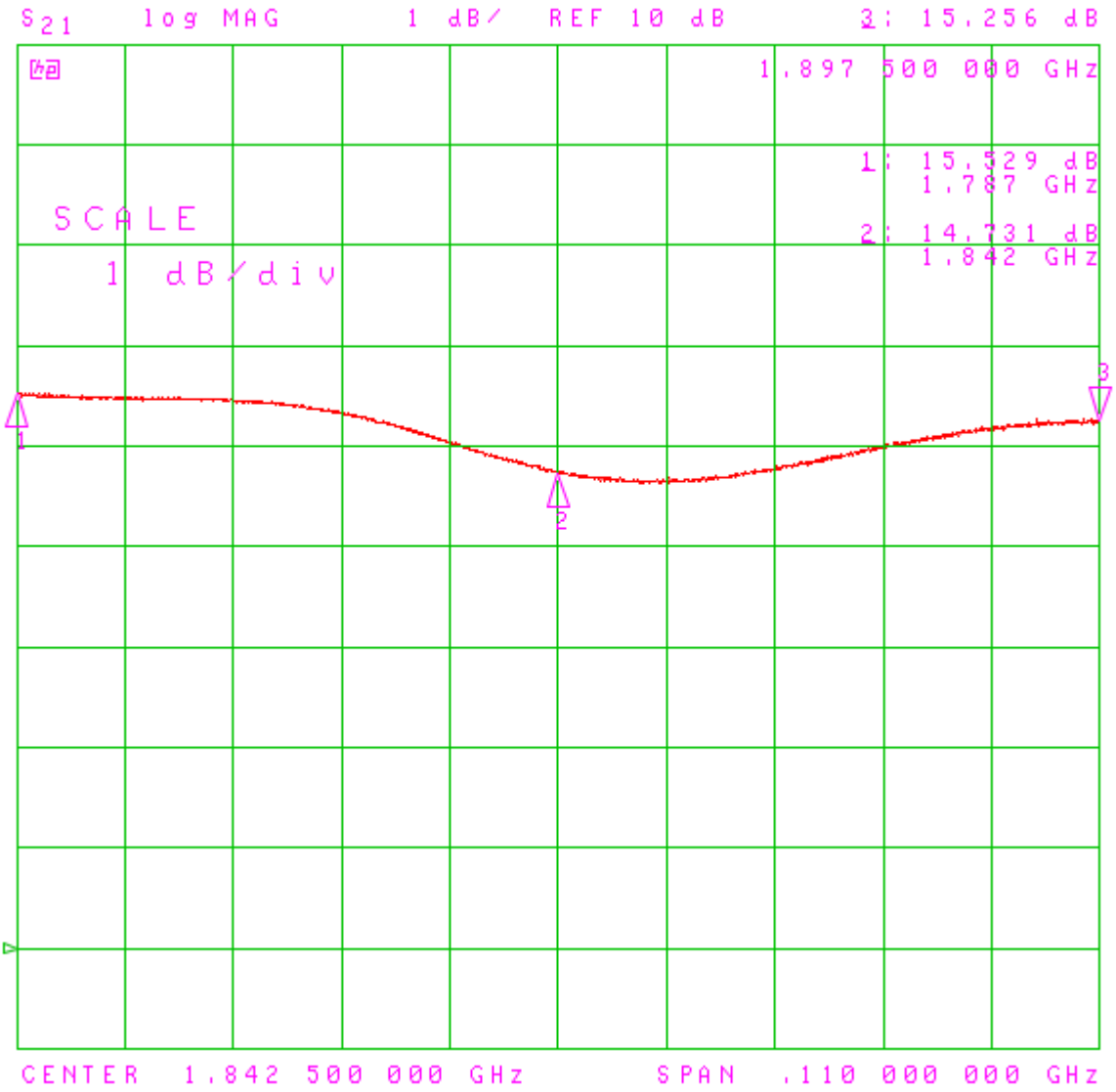

Figure 4.4. First stage amplifier 2

The following two figures (Fig. 4.5 and 4.6) are the amplifiers under test for the reasonable distortion configuration. Coincidentally, these two are the same model as the first stage amplifiers. The first stage amplifiers put these two nearly 7 dB beyond their 1 dB compression point. While the amplifiers are heavily saturated, their characterizations show that their output responses are nearly identical, representing only a minor calibration challenge.

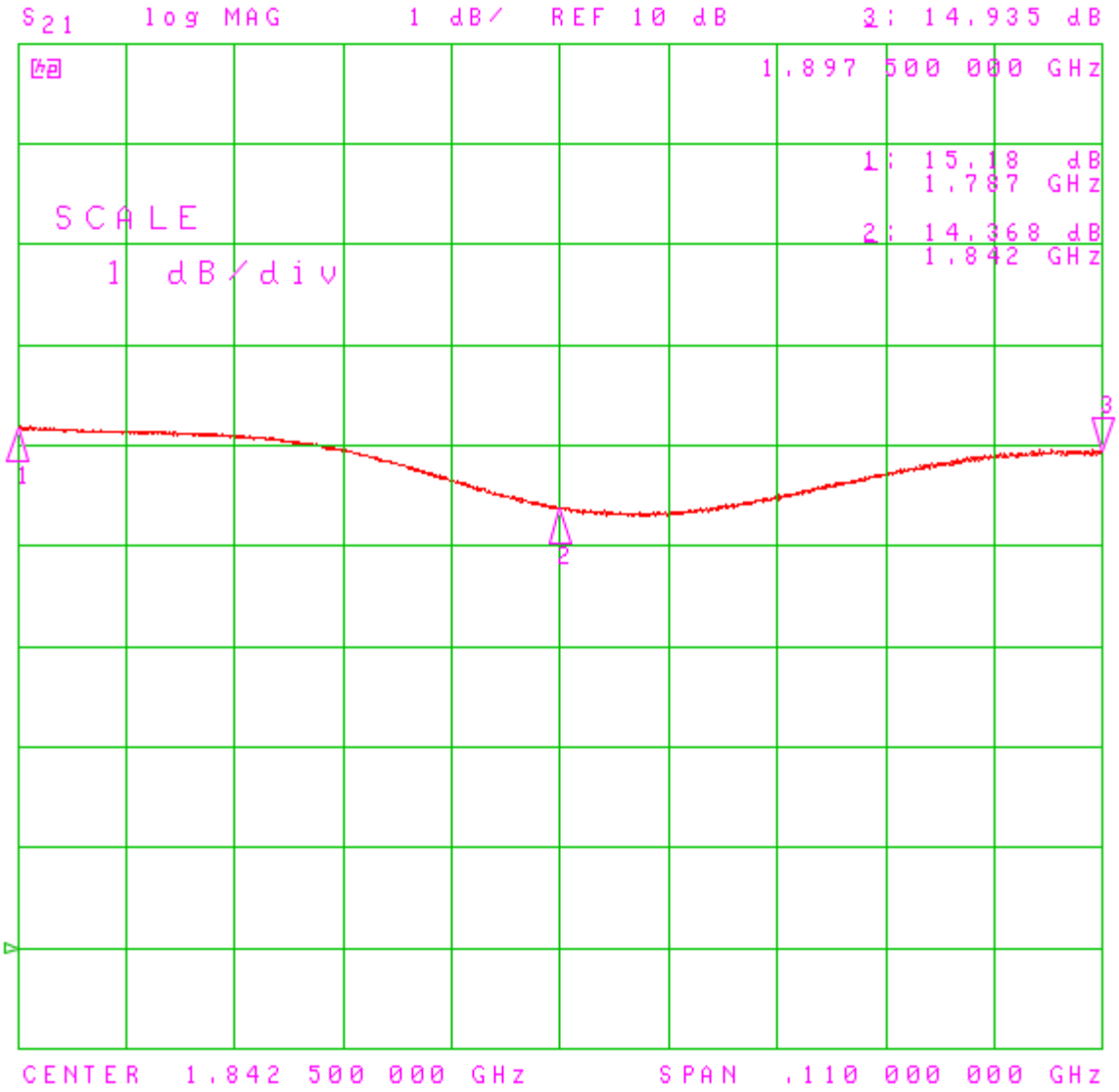

Figure 4.5. In-band amplifier 1

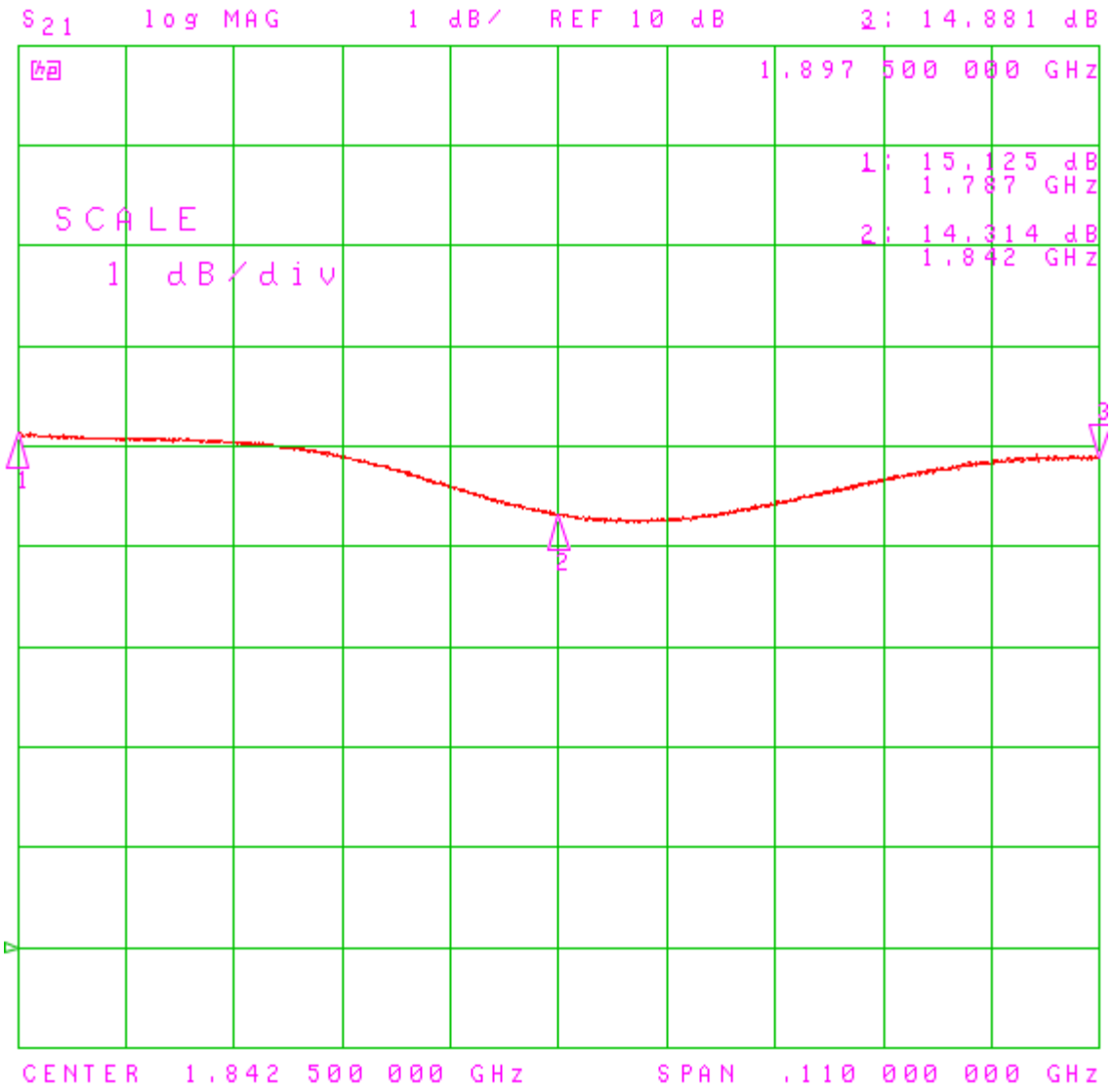

Figure 4.6. In-band amplifier 2

The final transmitter configuration (see Fig 5.15) provides a worst case scenario for amplifier mismatch and saturated distortion. This configuration is purposefully worse than what would be encountered in a reasonable real-world application. This pair of amplifiers are being operated over 600 MHz out-of-band. At the band of operation, they actually serve as attenuators rather than amplifiers, although the output power is relatively unimportant for the purpose of this experiment. What is important to note from the following two figures is how wildly different their output response is at this frequency band, this presents a definite calibration challenge. There is a nearly 3 dB mismatch at the center frequency. Obviously, the LINC approach is best

implemented with two nearly identical PA's. However, the experimental results presented in Section 5.3 with this configuration speak to the robustness of this system and process.

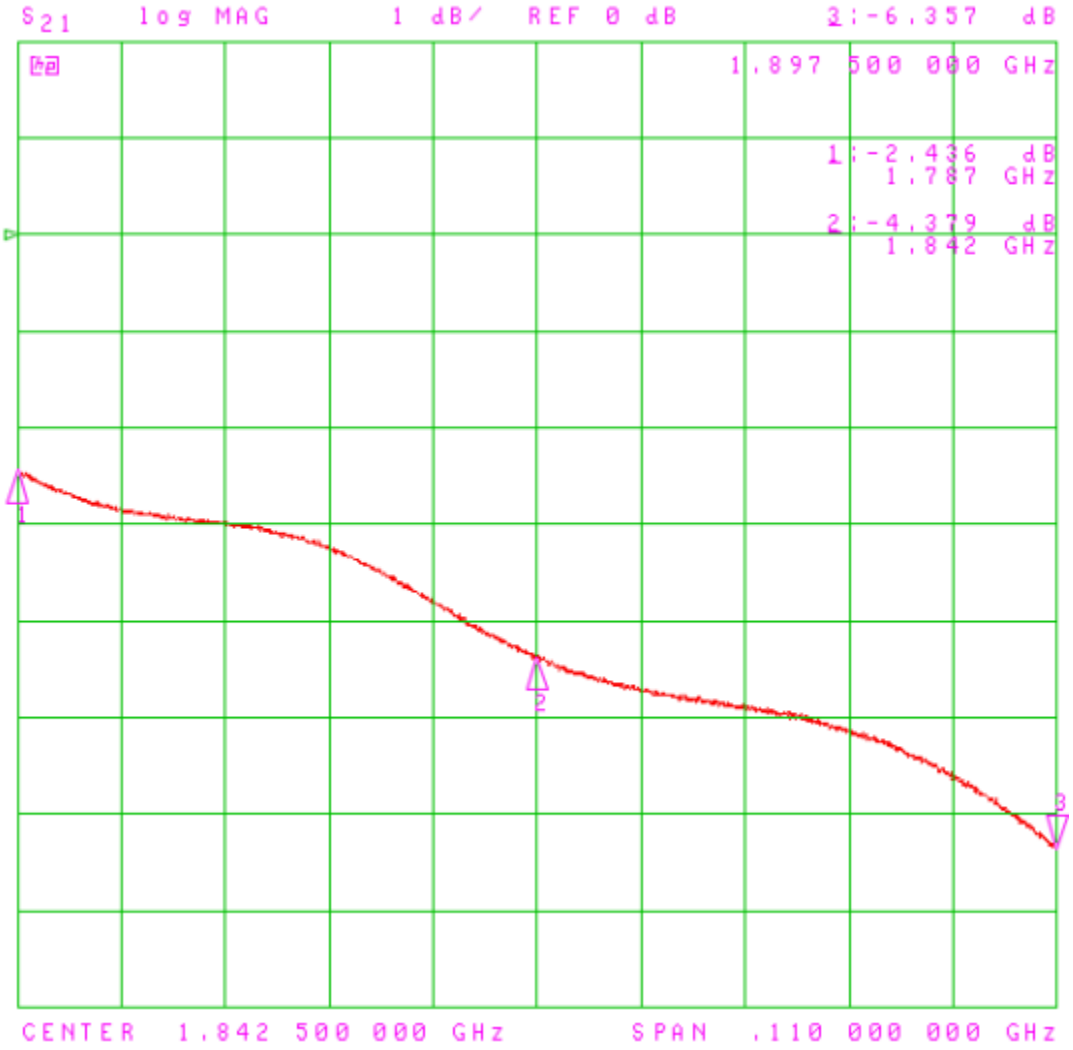

Figure 4.7. Out-of-band amplifier 1

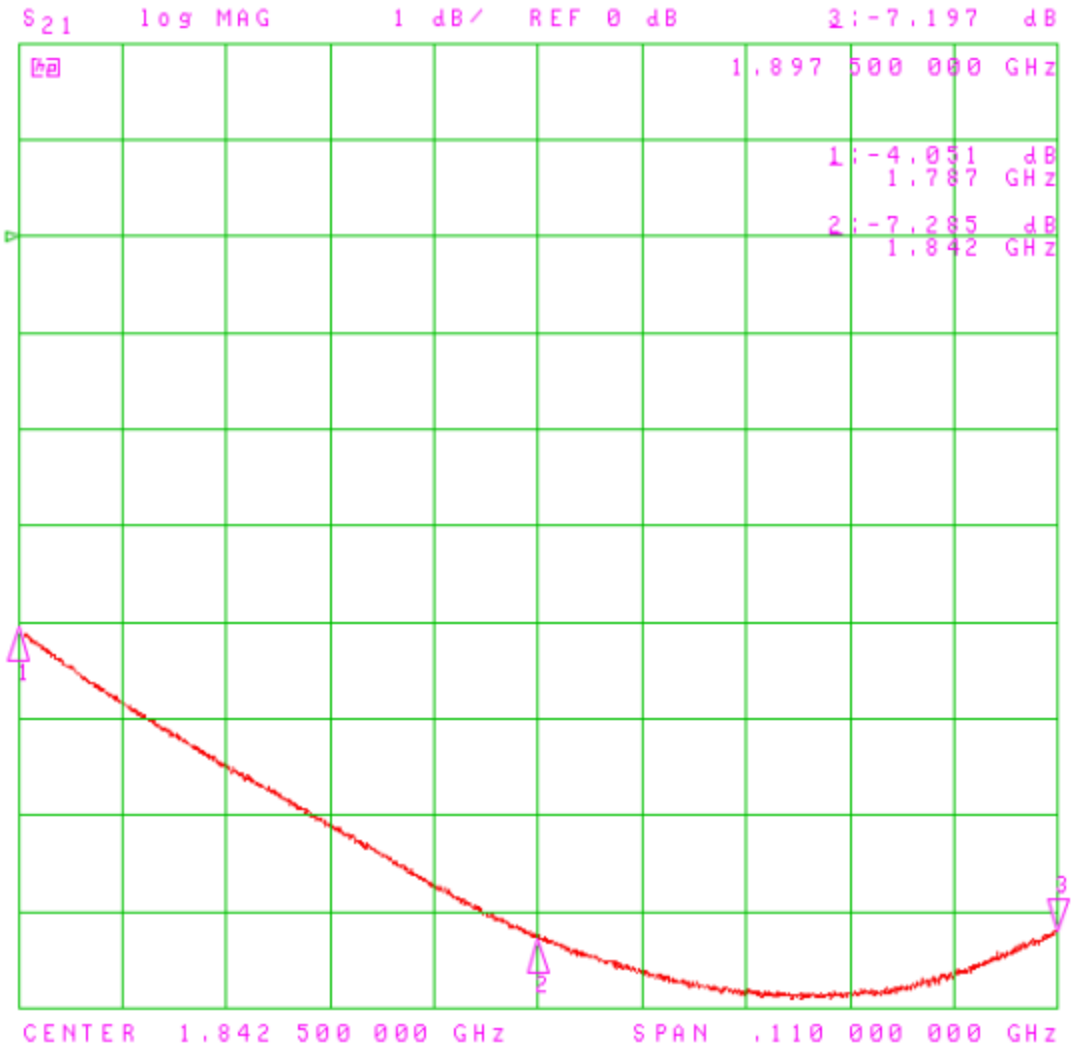

Figure 4.8. Out-of-band amplifier 2

5 Performance Results

This section is presented as the results from four separate hardware configurations. Each set of data includes: the received waveform amplitude, the autocorrelation of an LFM chirp compared to the simulation optimized NLFM waveform, the autocorrelation of the simulation optimized NLFM compared to the hardware-in-the-loop optimized NLFM, the transmitted spectral content of an LFM chirp, the transmitted spectral content of the simulation optimized NLFM waveform, and the transmitted spectral content of the hardware-in-the-loop optimized NLFM waveform. All data sets are utilizing a 64 chip and 64 size constellation PCFM waveform.

5.1 Four Chip Taper – No Transmitter Amplifiers

This configuration has the signals coming directly from the arbitrary waveform generator into the hybrid coupler. Since there are no transmitter power amplifiers, this represents the ideal case with the least amount of waveform distortion. Shown below is the transmitter configuration (figure does not include the signal generator providing the external trigger).

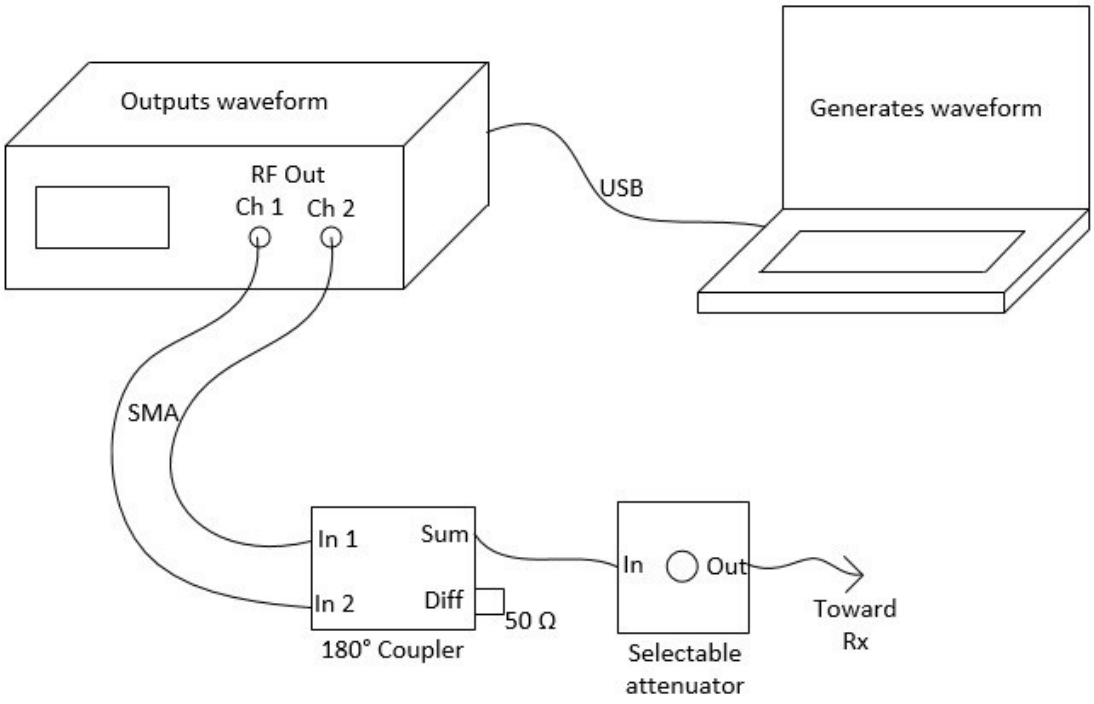

Figure 5.1. Transmitter configuration, no amplifiers

The following three figures all come from data sampled in the receiver digitizer and then processed in Matlab.

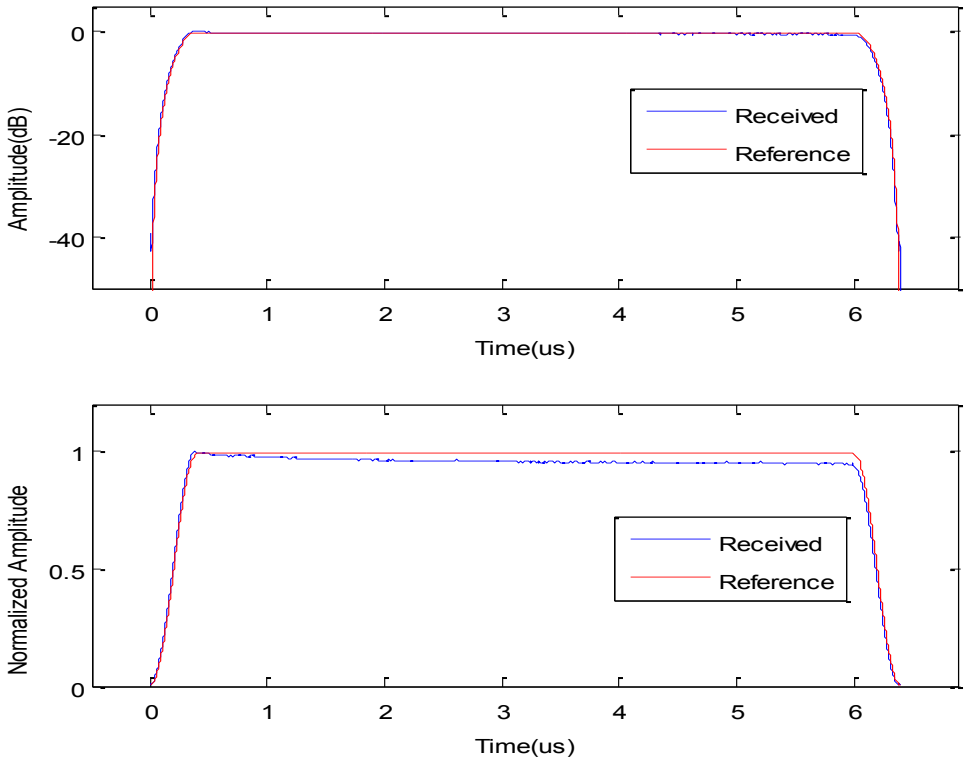

Figure 5.2. Amplitude of received pulse

The red line corresponds to the ideal amplitude with a 4 chip transition length for the Tukey window. The slight mismatch that can be seen in the linear scale is probably attributed to reflections or some components in the receiver attenuating the higher frequency portion of the waveform. Still, it is a very clean waveform sampled by the digitizer.

The following table gives the metrics of the optimization parameter, peak sidelobe level of the autocorrelation, for the three utilized waveforms.

Table 5.1. PSL performance, no amplifiers

	PSL
LFM chirp	-14.56 dB
Simulation optimized waveform	-42.85 dB
Hardware-in-the-loop optimized waveform	-43.70 dB

Clearly, there is a vast improvement in the PSL metric when going from the LFM waveform to the simulation optimized waveform. The improvement in hardware optimization is modest but does manage to improve the waveform on the PSL metric.

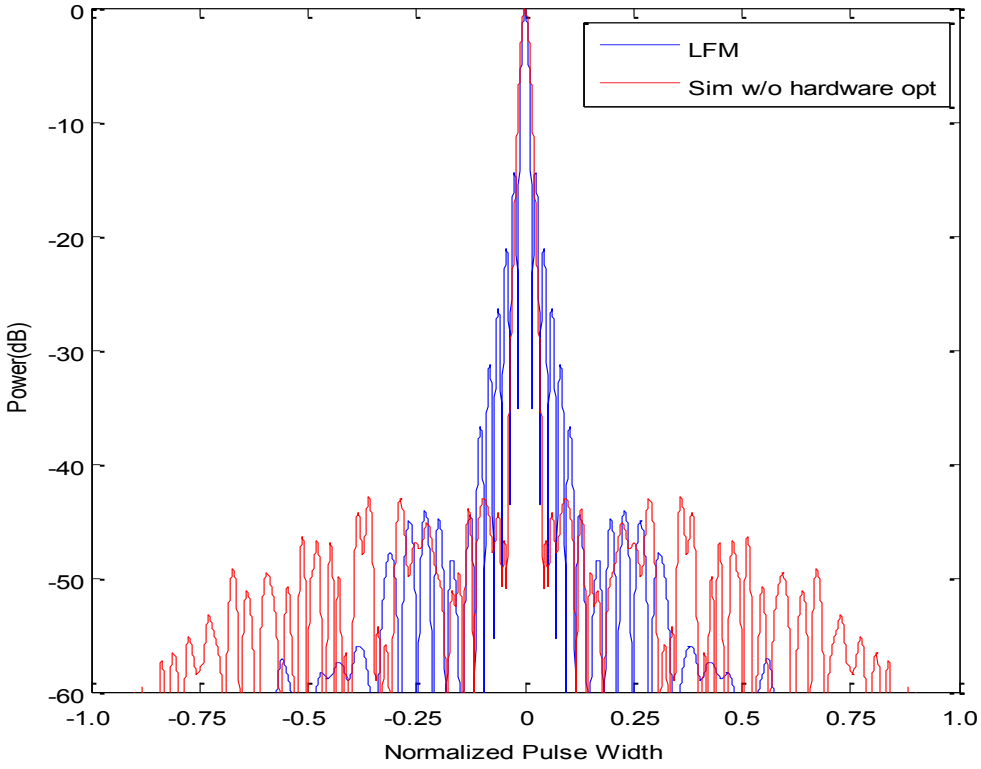

Figure 5.3. LFM and simulation optimized PCFM

The previous figure shows the autocorrelation of an LFM chirp, which was used as the optimization routine seed, compared to the simulation optimized waveform. Similarly, the figure below shows the autocorrelation of the simulation optimized waveform, which was used as the optimization routine seed, compared to the hardware-in-the-loop optimized waveform.

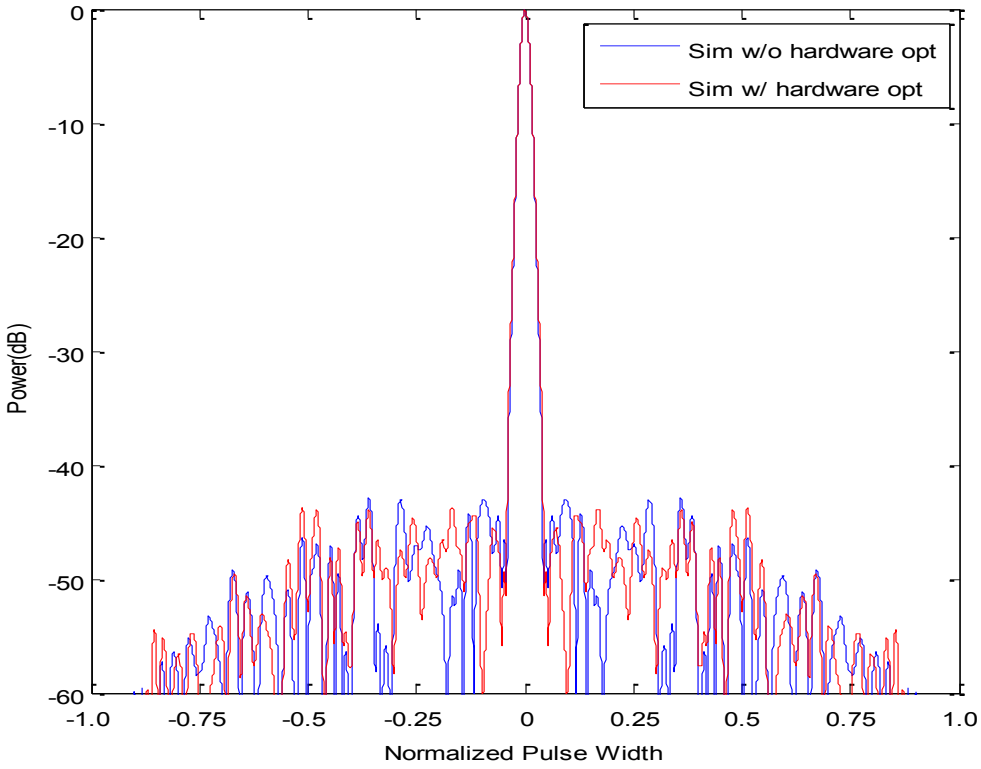

Figure 5.4. Simulation optimized PCFM and hardware optimized PCFM

The next three figures look at the spectral content of the transmitted waveforms. The data is captured with a real time spectrum analyzer. The maximum span of the real time spectrum analyzer is only 110 MHz. However, this is deemed sufficient by observing that the spectral content goes down below the noise floor within that span. The stand-alone trace in each figure represents the spectral content without the Tukey window applied. The trace accompanied by the real-time shading represents the spectral content with the Tukey window applied. This is where

the value of the LINC approach can be observed. The spectral roll-off is suppressed by over 20 dB. The out-of-band spectral power is certainly more than 60 dB below the peak power. This is accomplished with only a four chip width taper. The spectral containment behaves roughly the same across all three waveforms, shown in the following three figures.

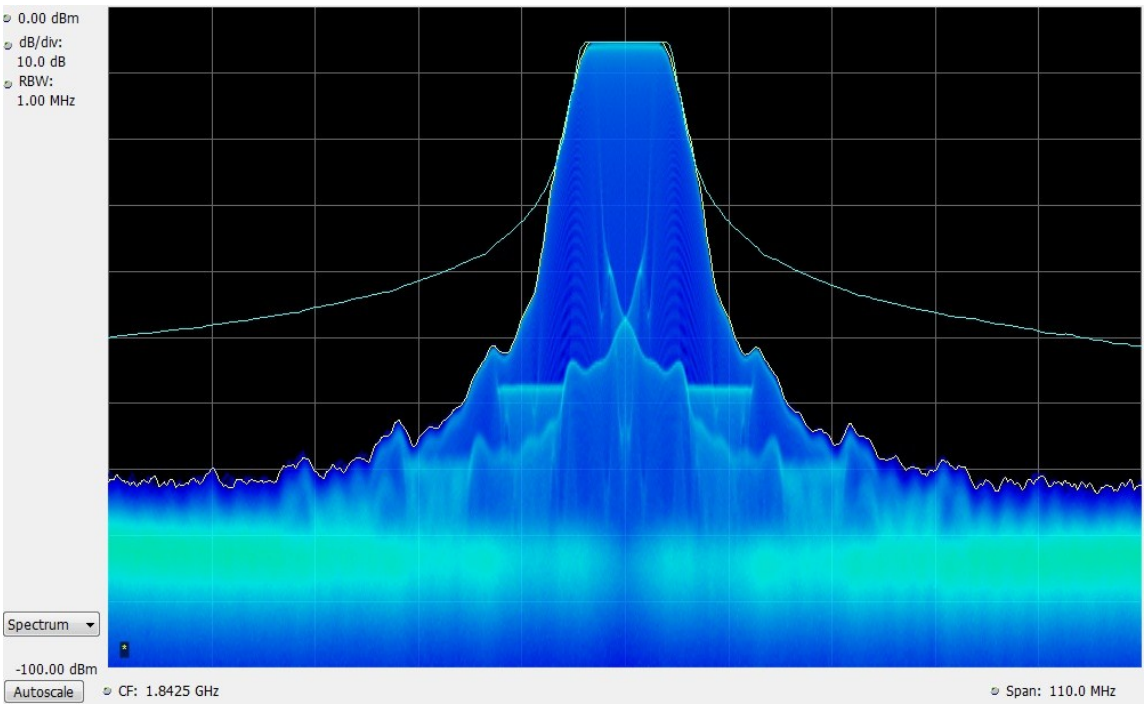

Figure 5.5. LFM transmitted spectrum

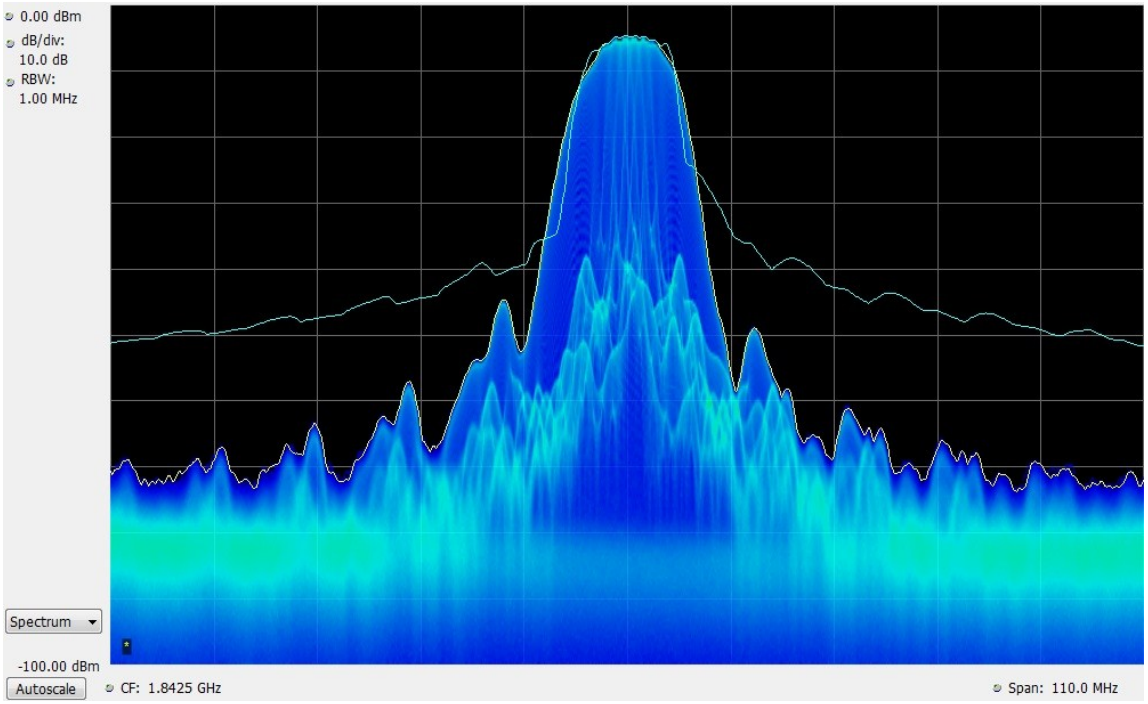

Figure 5.6. Simulation optimized PCFM transmitted through hardware

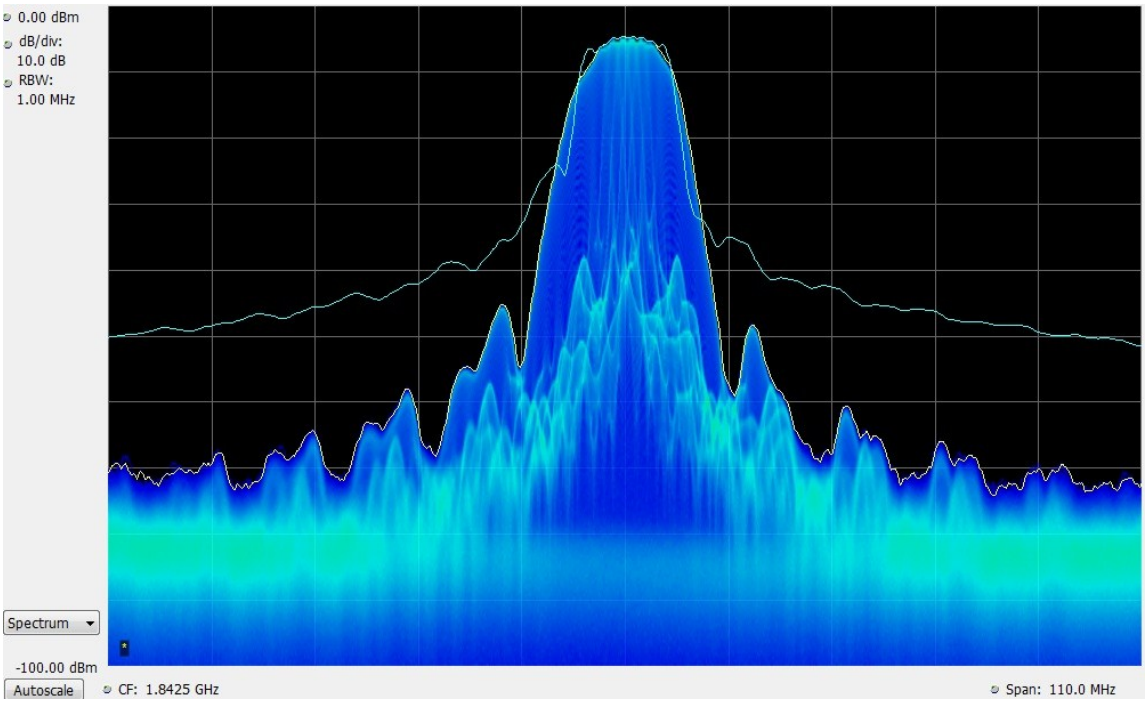

Figure 5.7. Hardware optimized PCFM transmitted spectrum

5.2 Four Chip Taper – In-band Transmitter Amplifiers

The next data set represents the in-band transmitter power amplifiers. The maximum output power of the arbitrary waveform generator was not sufficient to put the amplifiers into saturation. Due to this, a two stage amplification was used with the first pair of amplifiers increasing the incident power at the second pair of amplifiers to roughly 7 dB past their 1 dB compression point. This ensured that the second pair of amplifiers were well into saturations. All four amplifiers used in this configuration were the same model and exhibited nearly identical output curves (see Figs 4.3-4.6). The configuration is shown below.

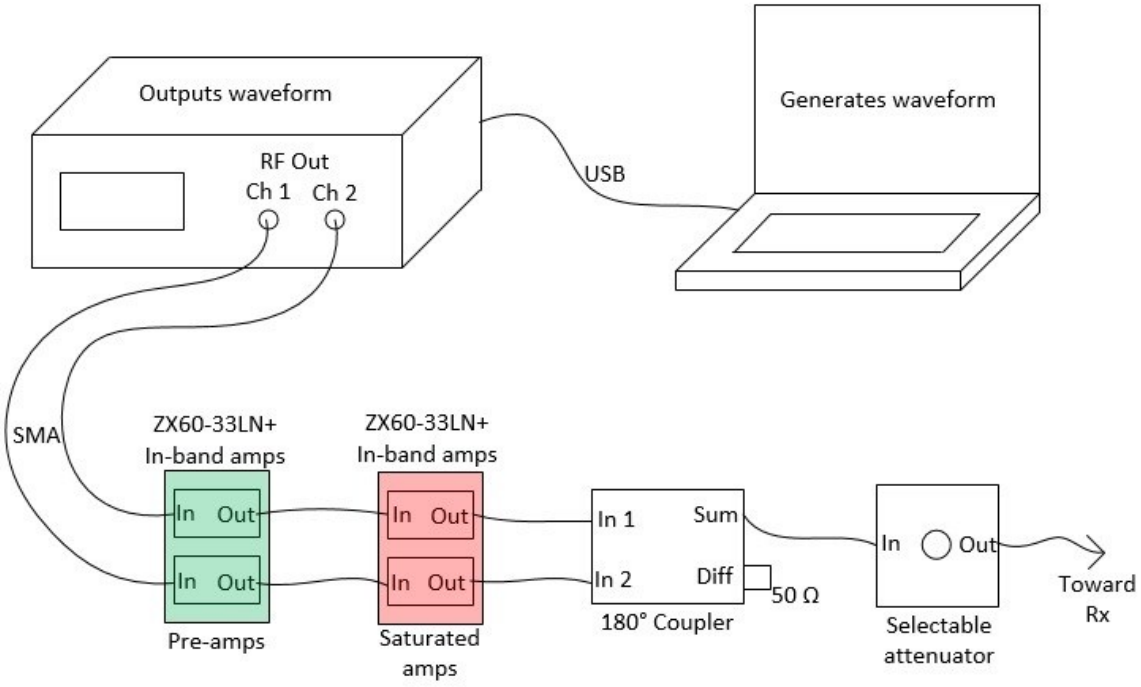

Figure 5.8. Transmitter configuration, in-band amplifiers

It is worth comparing the following amplitude figure with Figure 5.2. The received waveform amplitude in the configuration without the power amplifiers is obviously better. The degradation seen below is introduced by the heavily saturated power amplifiers. However, the amplitude taper at the beginning and at the end of the pulse is still well defined.

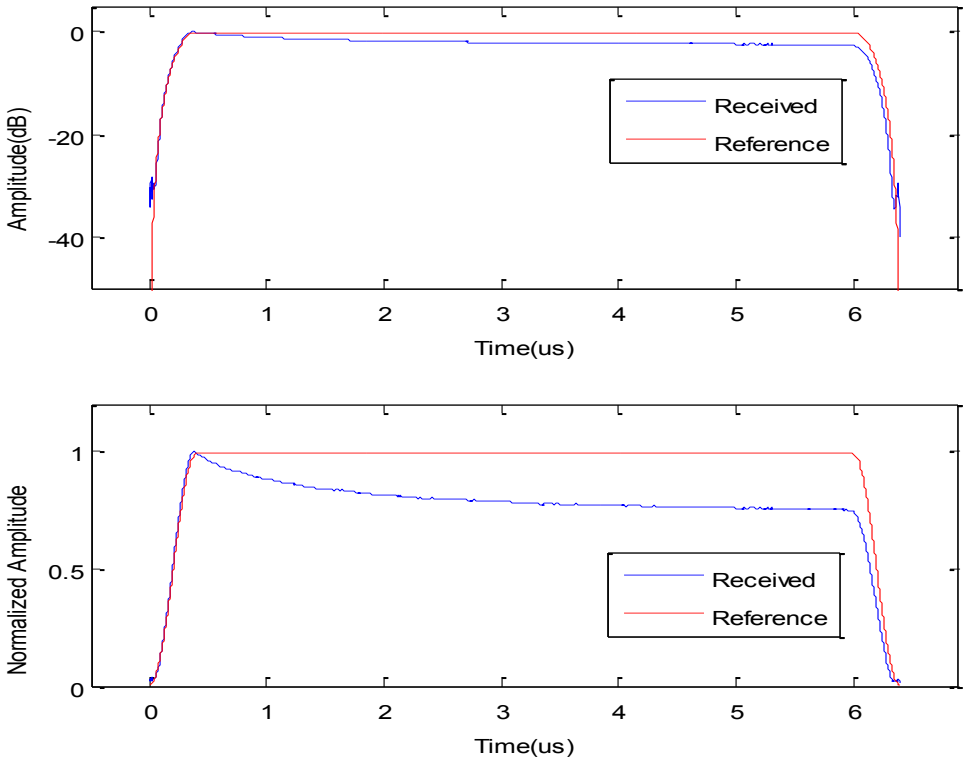

Figure 5.9. Amplitude of received pulse

Due to the added distortion of the heavily saturated transmitter power amplifiers, it stands to reason that the PSL performance would be worse than those shown in Table 5.1 from the no amplifier configuration. Also due to this added distortion, it makes sense that hardware-in-the loop optimization stage gives a larger improvement to PSL in this configuration. This is observed. Only a 0.85 dB improvement was gained in the no amplifier configuration while a 1.47 dB improvement was seen here. The reason for this larger improvement is because there is simply a greater degradation in the simulation optimized waveform for the hardware-in-the-loop optimization stage to recover.

Table 5.2. PSL performance, in-band amplifiers

	PSL
LFM chirp	-13.66 dB
Simulation optimized waveform	-41.31 dB
Hardware-in-the-loop optimized waveform	-42.78 dB

The following autocorrelation comparisons are not significantly different from the autocorrelation comparisons of the no amplifier configuration.

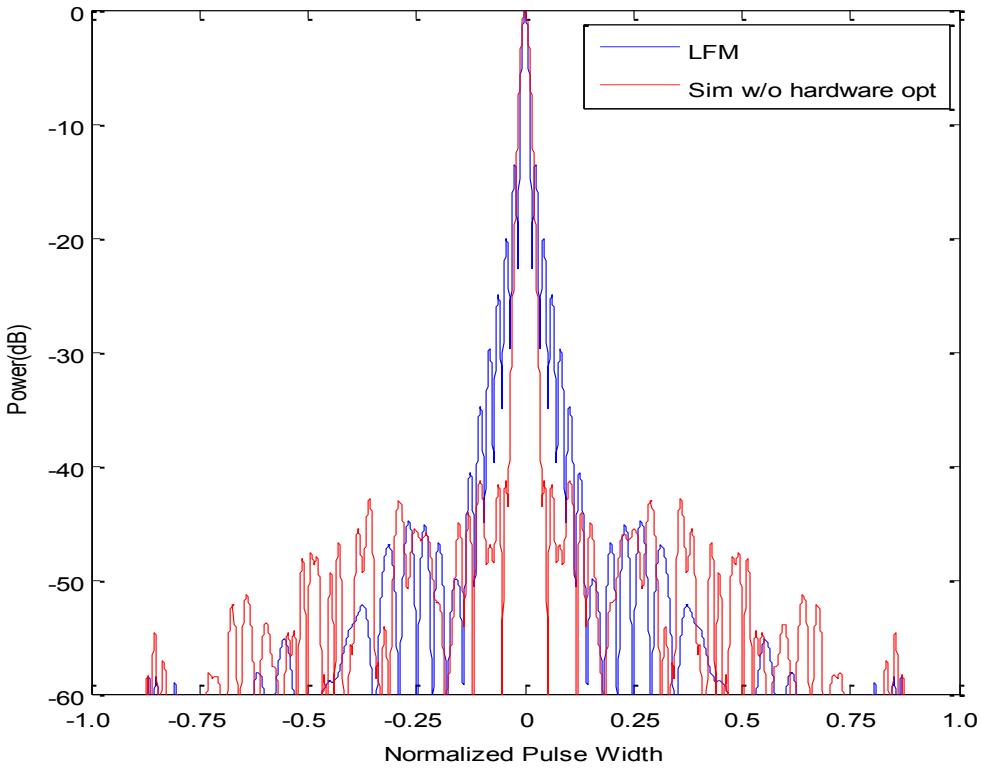

Figure 5.10. LFM and simulation optimized PCFM

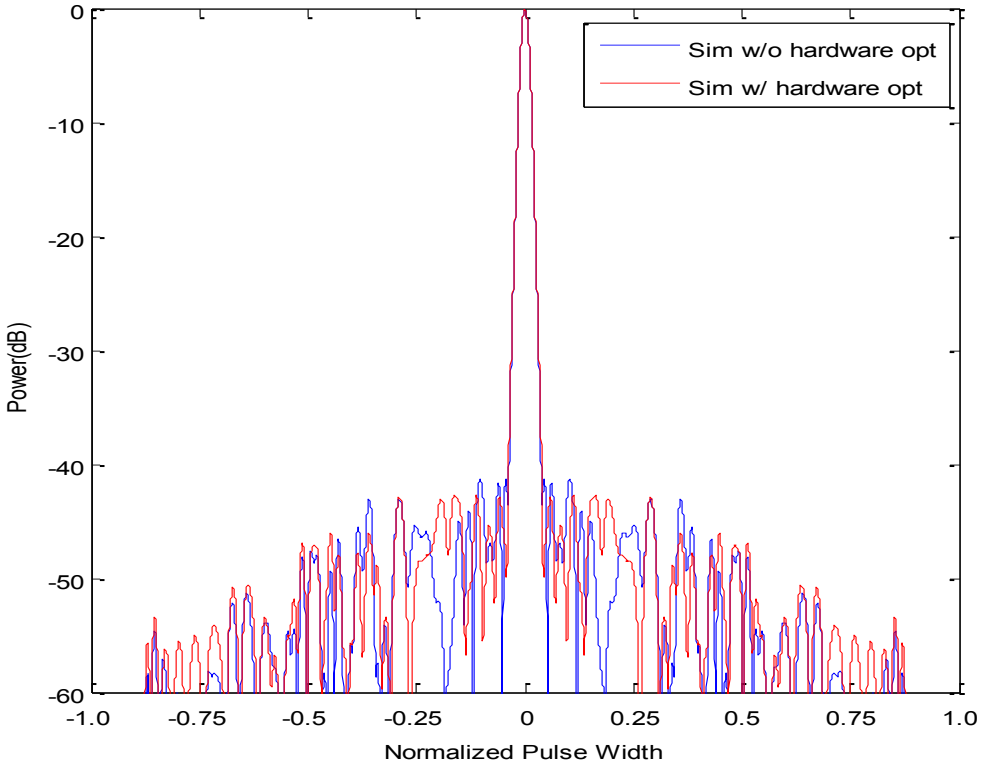

Figure 5.11. Simulation optimized PCFM and hardware optimized PCFM

Figures 5.5 through 5.7 form the best case baseline (no amplifiers) of the spectral containment of the transmitted waveform. This configuration (Figures 5.12 through 5.14), as expected, does not see quite the same roll-off. It is reasonably close though. The spectral content is still suppressed roughly 15-20 dB with the Tukey window applied compared to without the window applied. This is an excellent result given the heavy saturation of the transmitter power amplifiers.

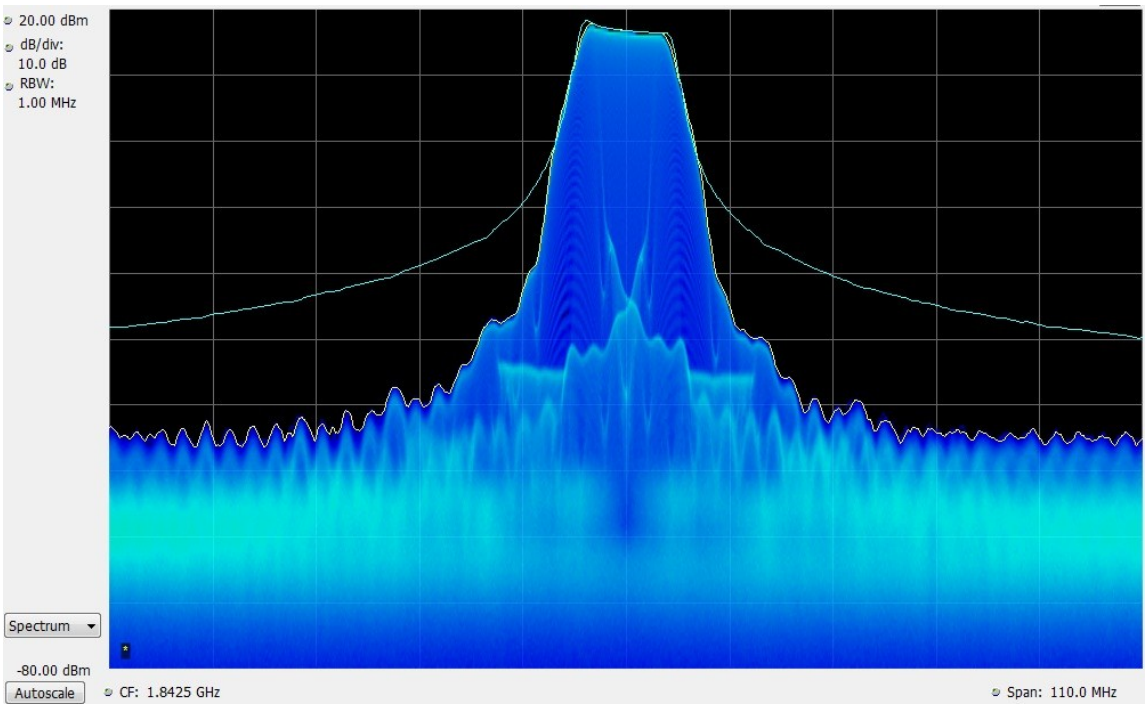

Figure 5.12. LFM transmitted spectrum

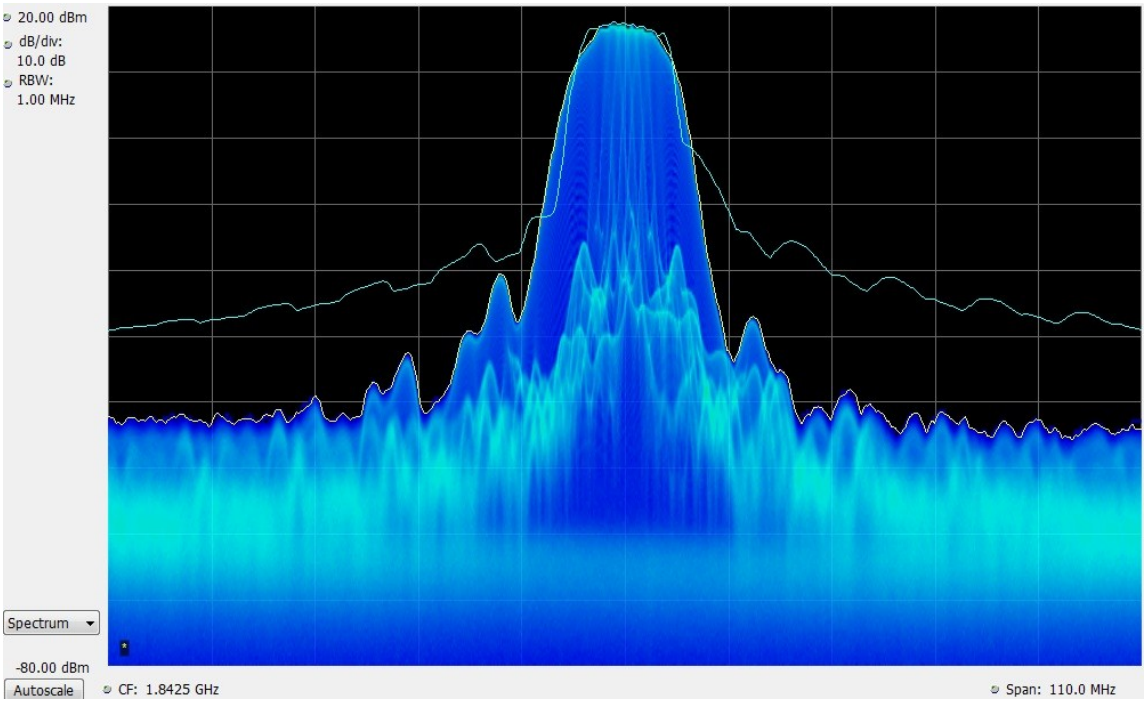

Figure 5.13. Simulation optimized PCFM transmitted through hardware

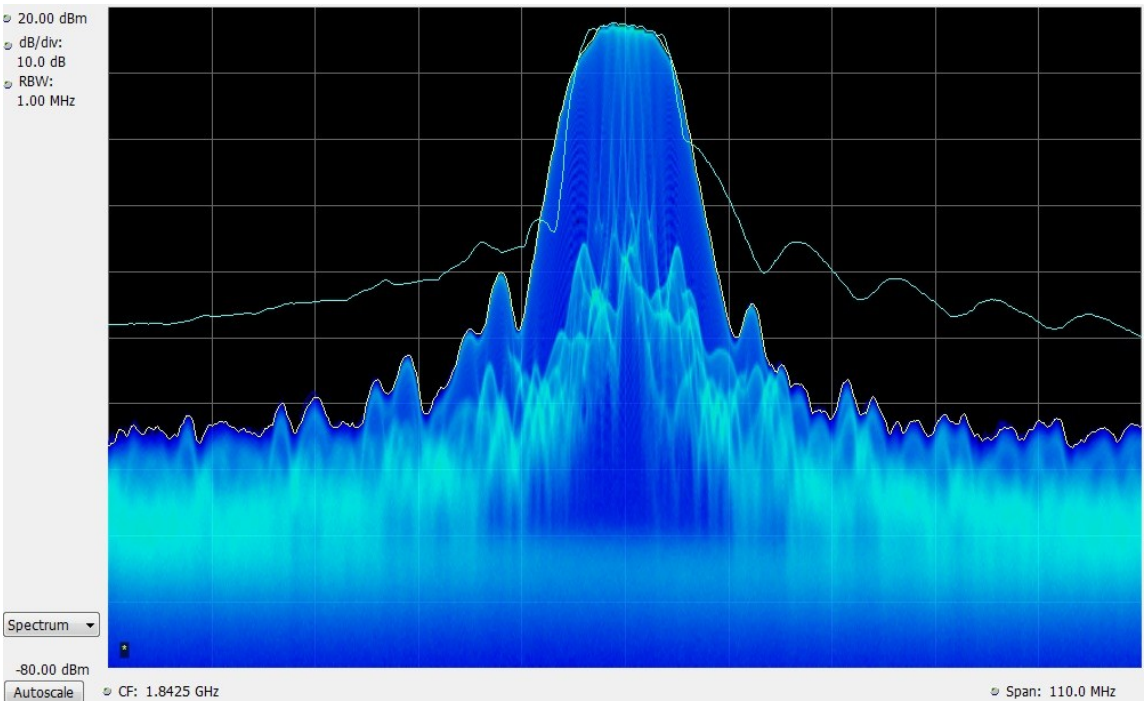

Figure 5.14. Hardware optimized PCFM transmitted spectrum

5.3 Four Chip Taper – Out-of-band Transmitter Amplifiers

The following configuration provides a worst case scenario with severe amplifier mismatch. The pair of power amplifiers used are nominally the same. However, the amplifiers are intentionally chosen to be out-of-band and their respective outputs are wildly different. Refer back to Figures 4.7 and 4.8 to see extreme differences between the two amplifiers. As with the previous configuration, a two stage amplification process is needed to ensure that the amplifiers under test are well into saturation. The configuration is shown below.

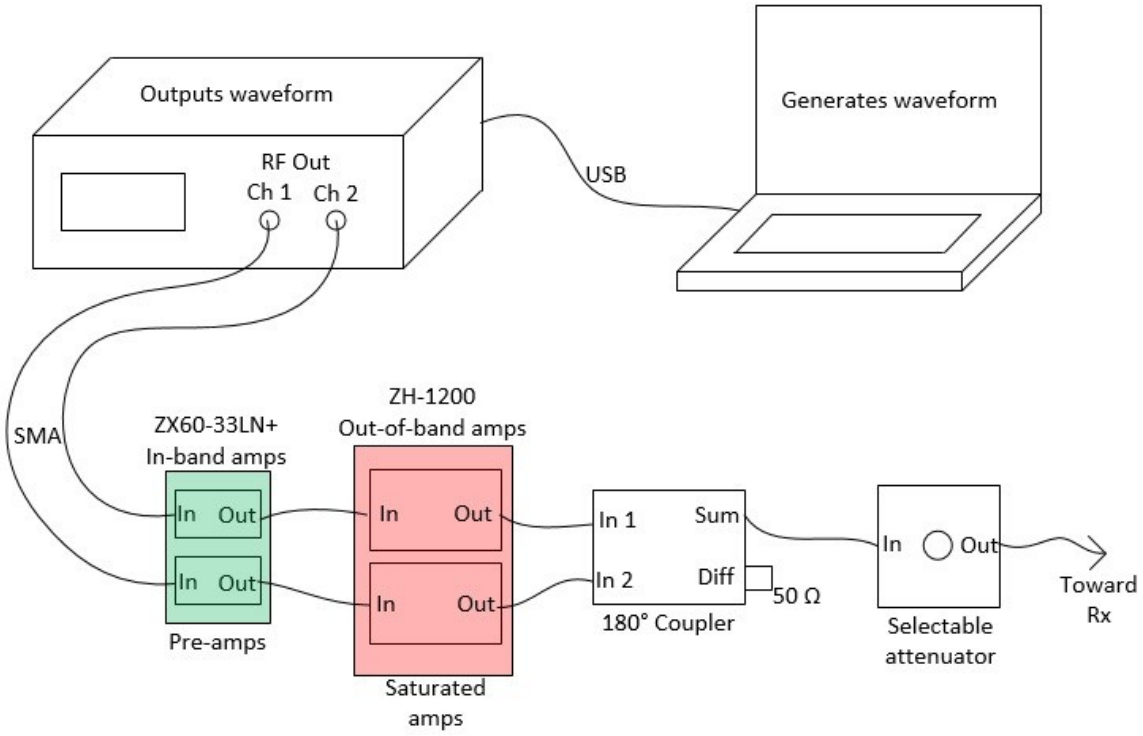

Figure 5.15. Transmitter configuration, out-of-band amplifiers

This configuration really shows off the robustness of this system and optimization process. The input power to each amplifier needs to be adjusted until their outputs match as closely as possible. This is necessary to get full cancelation when the waveforms are completely out-of-phase going into the hybrid coupler. This simple and straight-forward calibration is all that is needed to deal with the large amplifier mismatch.

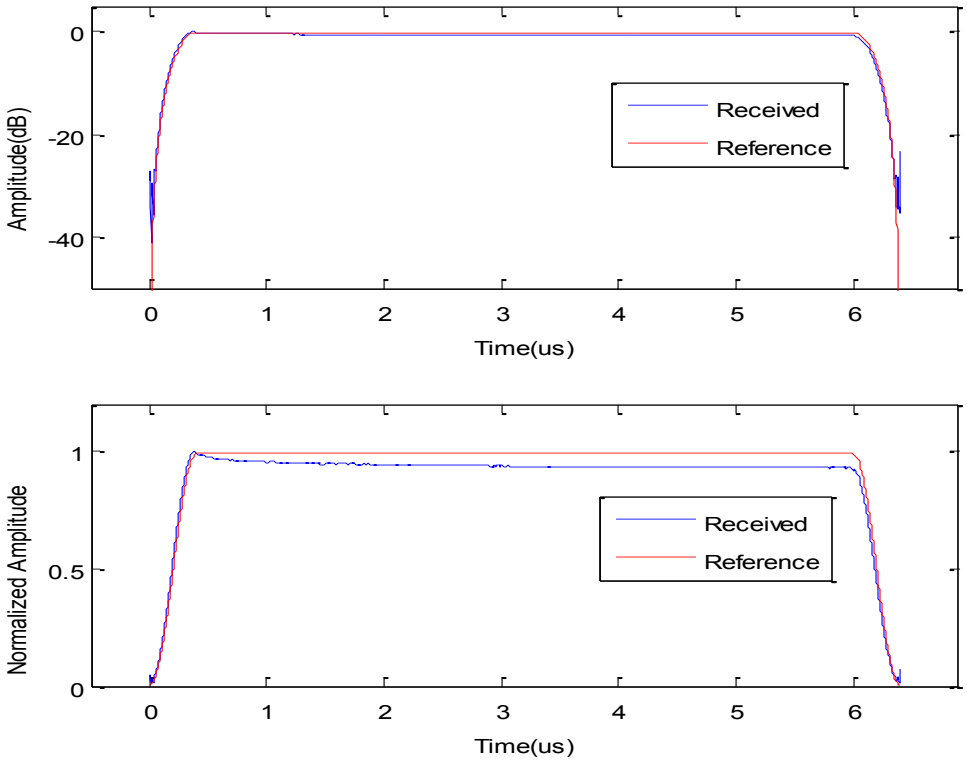

Figure 5.16. Amplitude of received pulse

After calibration, a good amplitude taper was achieved with cancellation at the extreme ends around -30 dB.

Table 5.3. PSL performance, out-of-band amplifiers

	PSL
LFM chirp	-14.51 dB
Simulation optimized waveform	-42.52 dB
Hardware-in-the-loop optimized waveform	-43.12 dB

The PSL performance was slightly better than the previous amplifier configuration but some of that likely comes from the fact that, after calibration, the amplifier output power was slightly higher than in the previous configuration. As expected, this configuration could not quite reach the mark of -43.70 dB set by the configuration without amplifiers. This set-up does a great job of showing how remarkably resilient this process is to transmitter amplifier distortion.

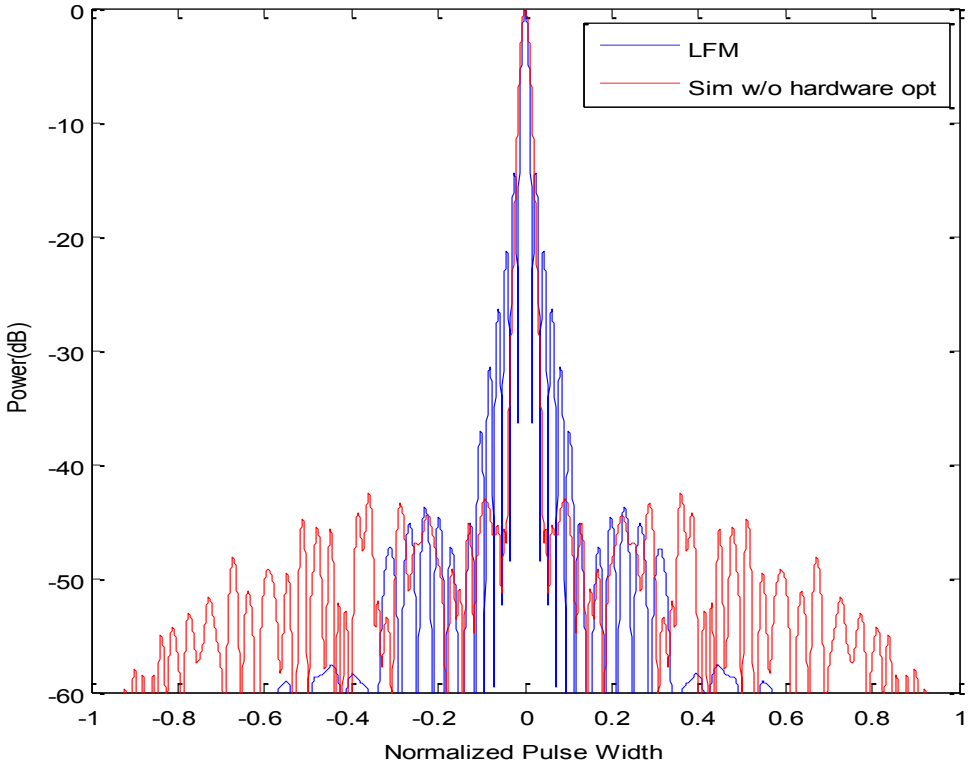

Figure 5.17. LFM and simulation optimized PCFM

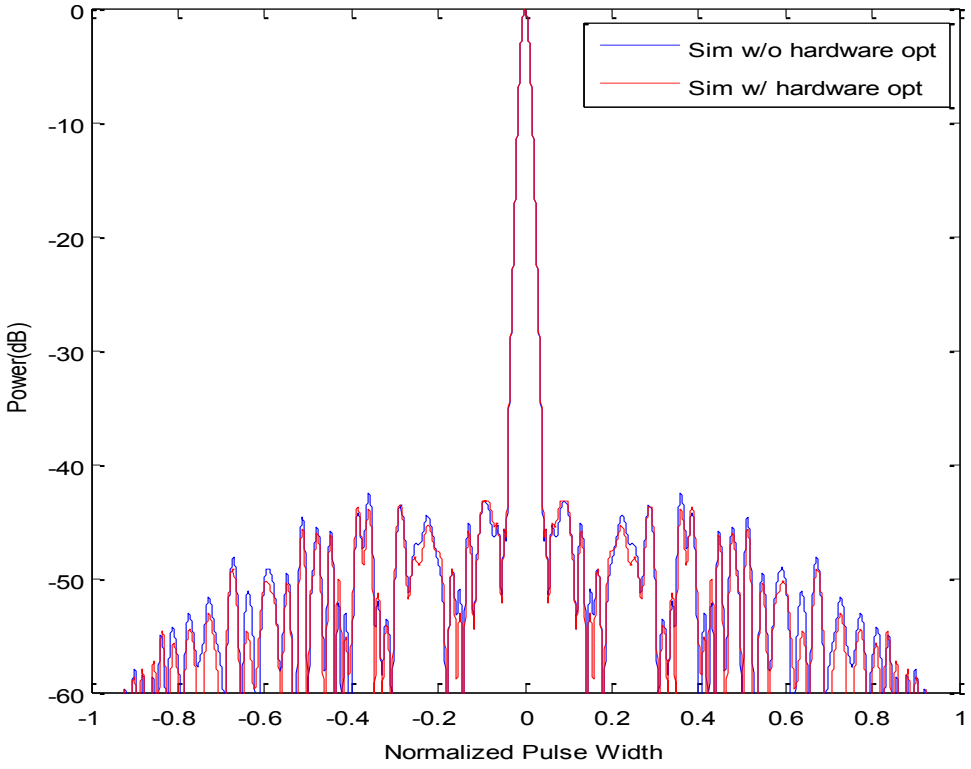

Figure 5.18. Simulation optimized PCFM and hardware optimized PCFM

The spectral content of this configuration compared to the previous two is a little dirtier but still shows that the amplitude taper is working as intended. Again, the amplifiers under test are over 600 MHz out-of-band, so the spectral content not being quite so well defined could be expected.

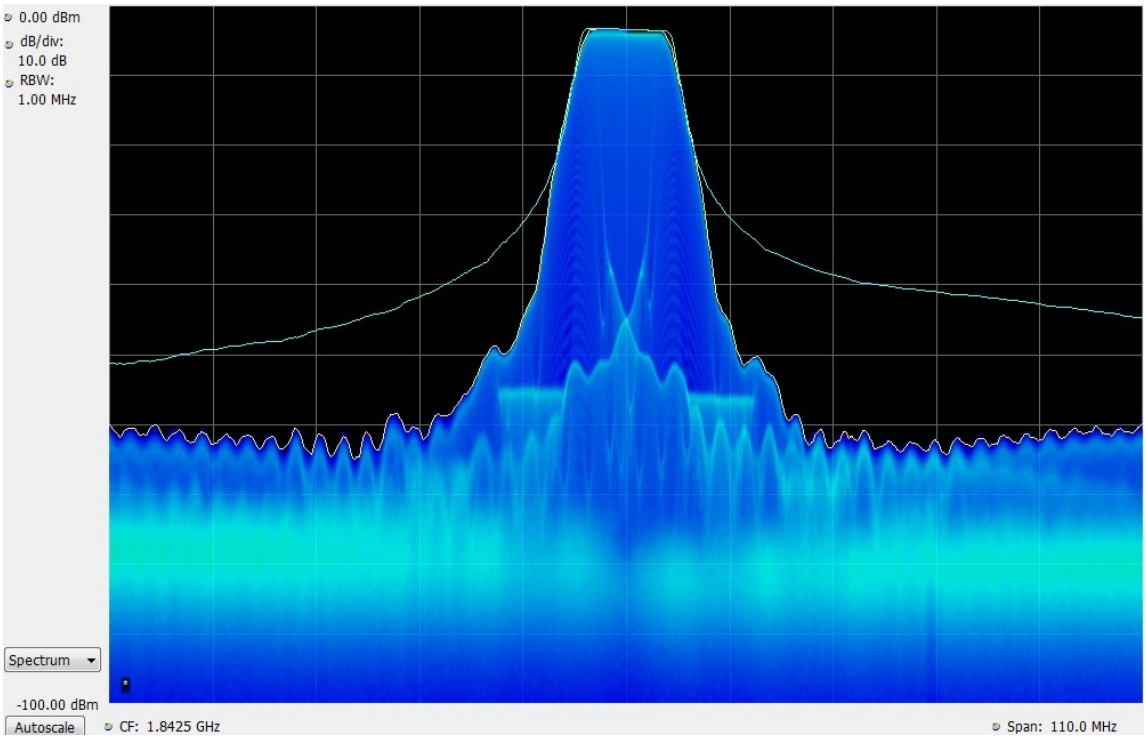

Figure 5.19. LFM transmitted spectrum

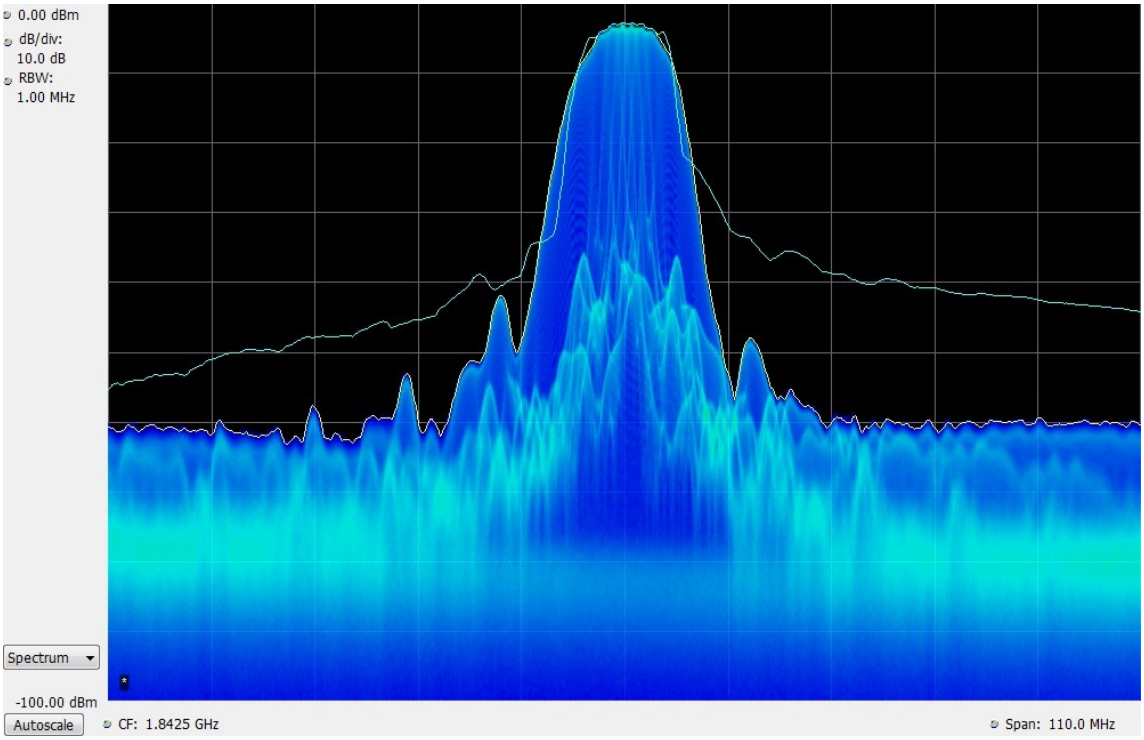

Figure 5.20. Simulation optimized PCFM transmitted through hardware

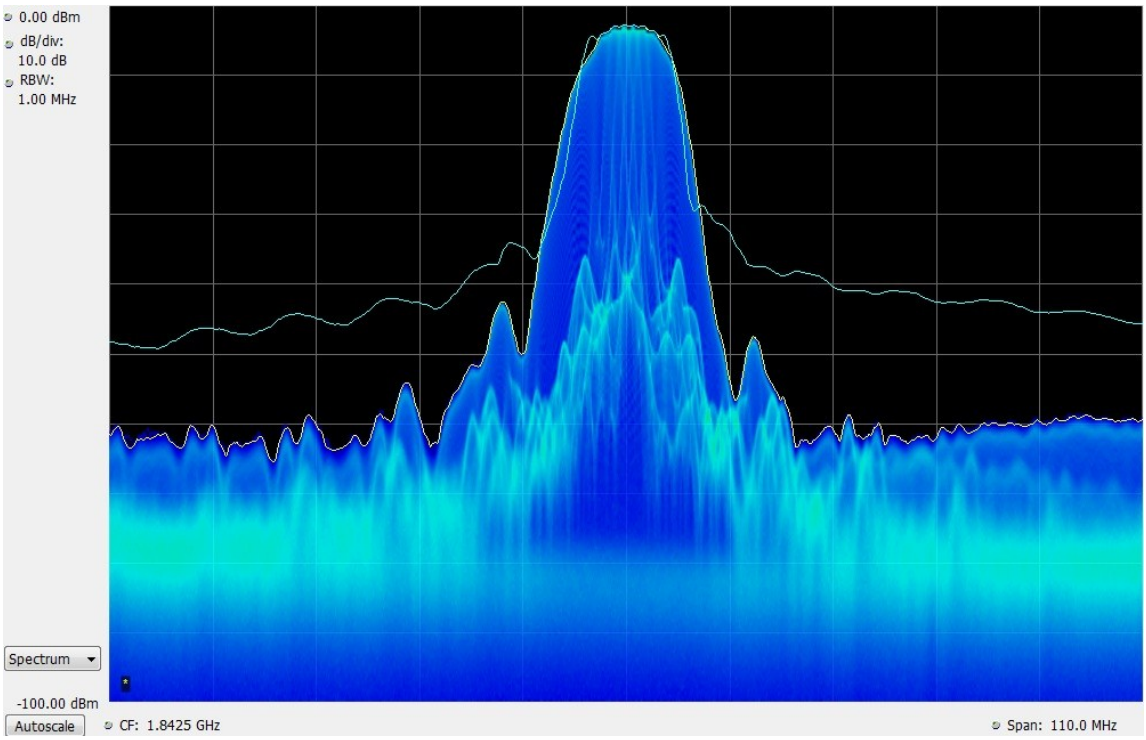

Figure 5.21. Hardware optimized PCFM transmitted spectrum

5.4 Sixteen Chip Taper – In-band Transmitter Amplifiers

This configuration is identical to the one presented in Section 5.2 and shown in Figure 5.8. The only difference is the taper transition length for the Tukey window is now 16 chips long, compared to 4. Of course this comes at a cost to decreased power efficiency and reduced SNR, since the two waveforms are out-phase-for a longer period of time. Depending on the application, the increased spectral containment might be required, and the trade-offs simply tolerated. This process is incredibly flexible, the length of the taper fully adjustable depending on the specific spectral requirements for a given application. It is a straight-forward spectral containment/SNR trade-off, refer back to Table 3.1 for the numerical breakdown.

The following figure of the received pulse amplitude shows similar distortion as Figure 5.9, as expected, only with a longer amplitude taper. It gives a good visual representation of the spectral containment/SNR trade-off.

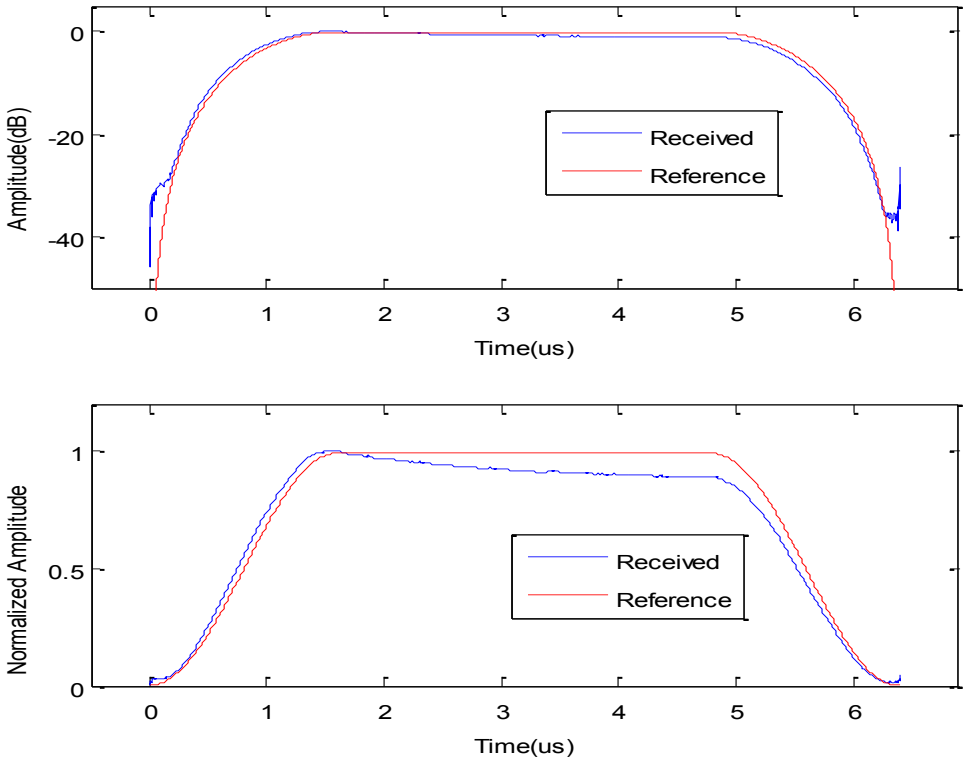

Figure 5.22. Amplitude of received pulse

Table 5.4. PSL performance, 16 chip taper

	PSL
LFM chirp	-16.38 dB
Simulation optimized waveform	-41.44 dB
Hardware-in-the-loop optimized waveform	-42.81 dB

The simulation optimized waveform is only 0.13 dB different from the 4 chip taper. The hardware-in-the-loop optimized waveform is only 0.03 dB different from the 4 chip taper result. This consistency was expected. Also, it is well established that windowing can have a positive effect on range sensitivity for LFM waveforms and this was observed with a nearly 3 dB improvement compared to the 4 chip Tukey window.

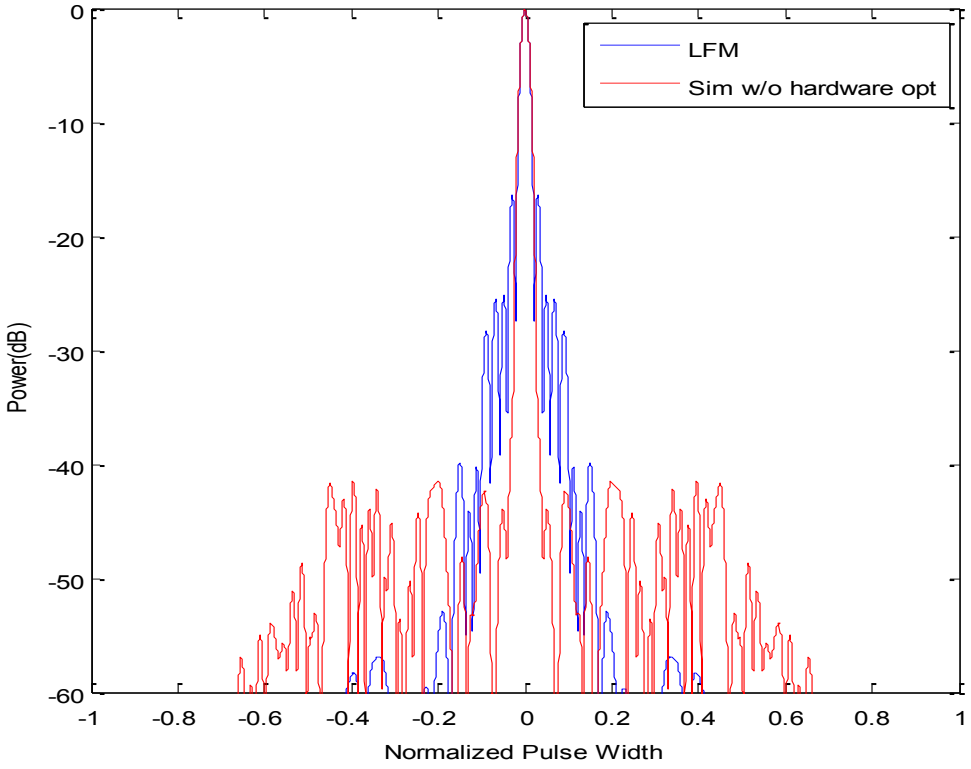

Figure 5.23. LFM and simulation optimized PCFM

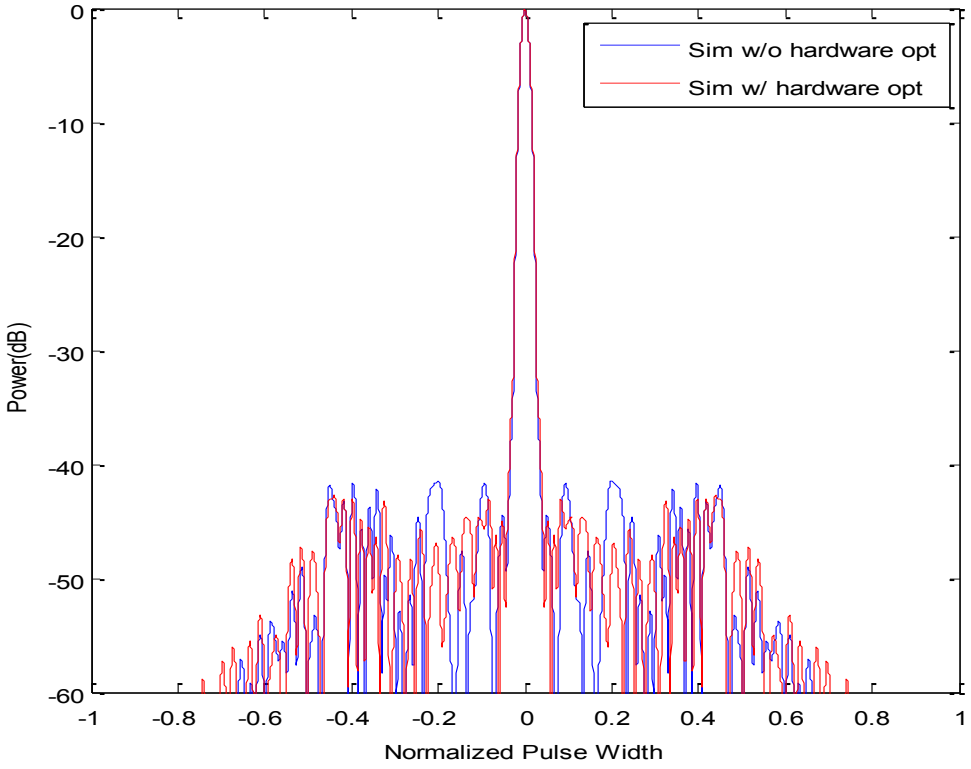

Figure 5.24. Simulation optimized PCFM and hardware optimized PCFM

The following three spectral plots should be compared back to Figures 5.12 through 5.14 to note the spectral advantage of using a longer taper length. The spectral roll-off is even sharper. The spectral content of the waveform reaches the noise floor very quickly. This data set was included to show versatility of this optimization process. Ideally, the minimum length taper that meets the specific spectral criteria for a given application would be utilized.

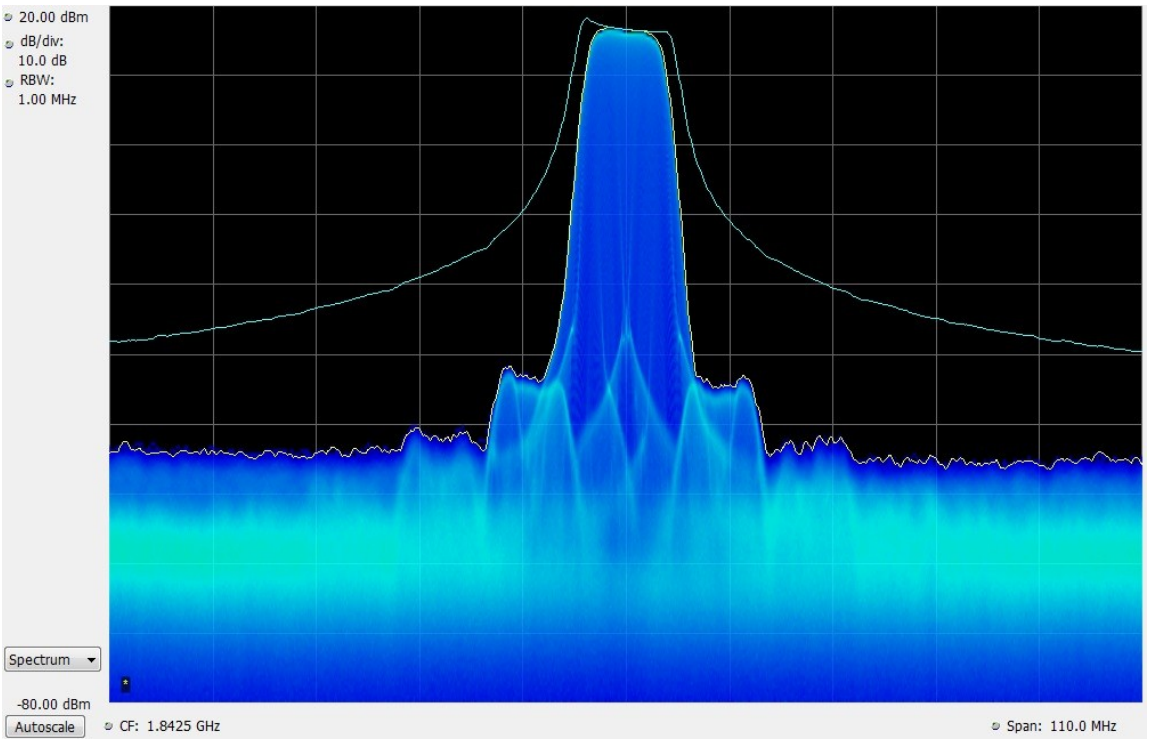

Figure 5.25. LFM transmitted spectrum

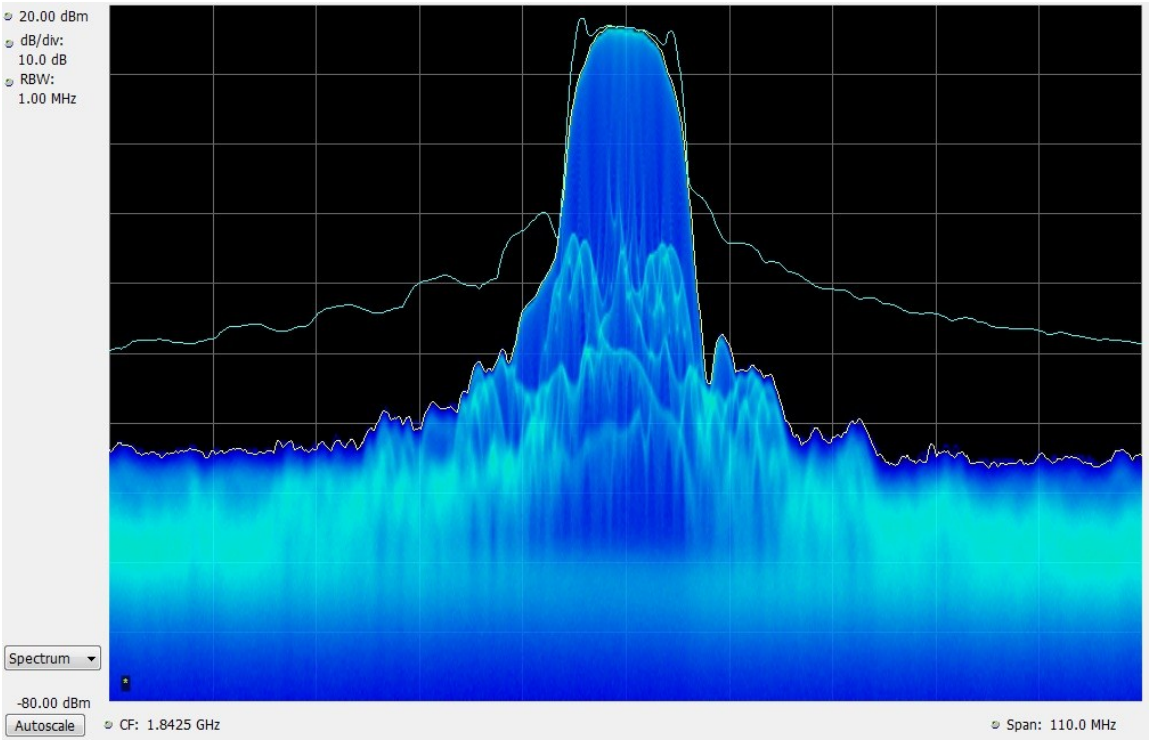

Figure 5.26. Simulation optimized PCFM transmitted through hardware

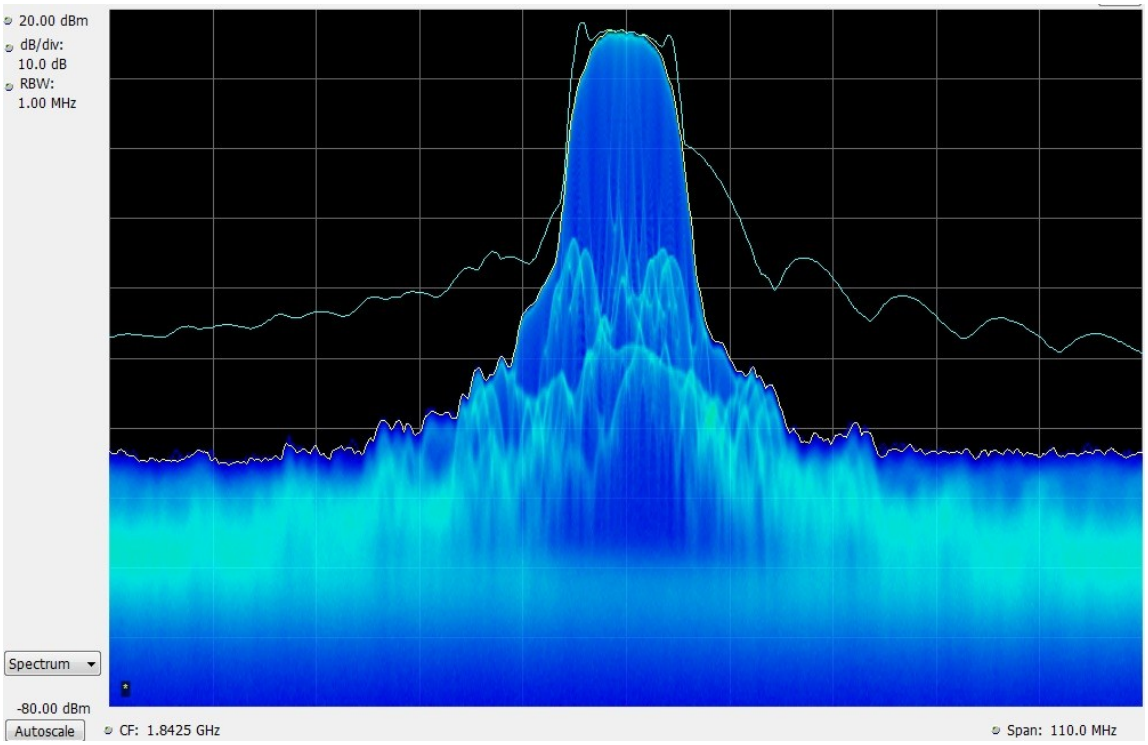

Figure 5.27. Hardware optimized PCFM transmitted spectrum

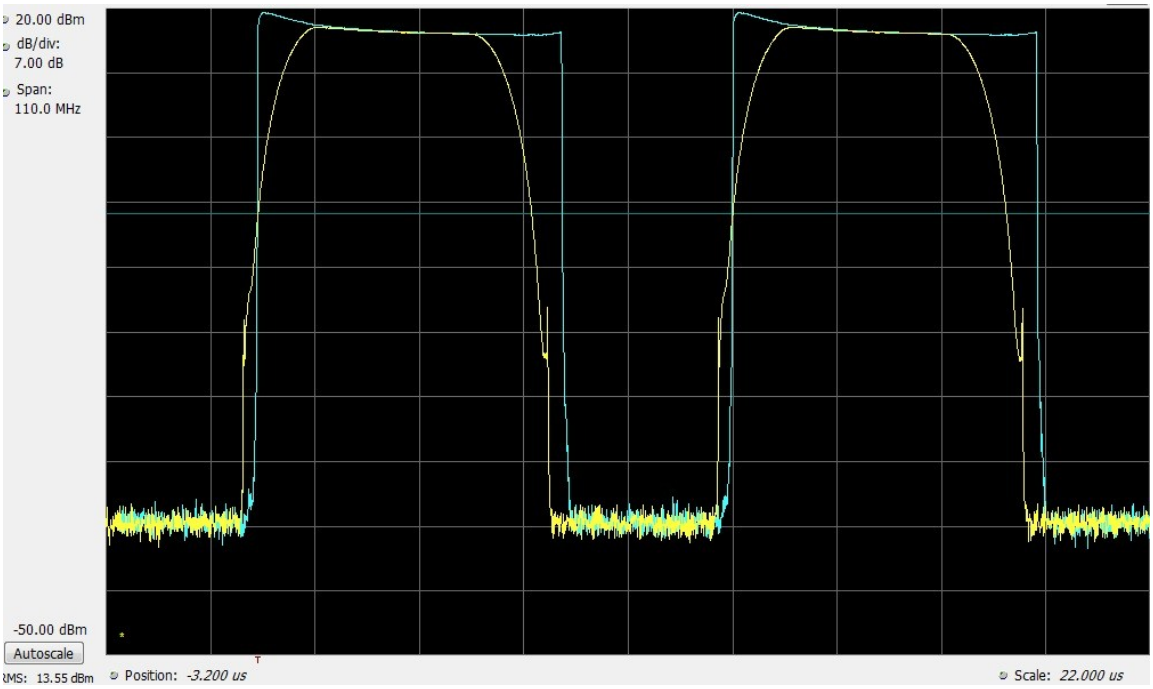

Figure 5.28. Transmitted pulses w/ and w/o taper

This final figure is the amplitude of the transmitted pulse in the time domain. The two traces represent with and without the Tukey window applied. The small time offset is only a result of the triggering. This compares reasonably well to all of the received pulse amplitudes.

6 Conclusion

6.1 Interpretation of Results

A robust waveform optimization scheme using the LINC approach was successfully developed. The experimental results support this claim. This process is resilient to transmitter PA distortion and mismatch, even in an extreme case. This process is also very flexible with regard to spectral containment. The implementation of the Tukey window makes it highly adjustable. In a real-world application, the minimum chip taper length that met a given set of spectral requirements would be chosen. This is easily accomplished with this process.

6.2 Suggested Improvements

This work only provided experimental results for one window type, and one modulation scheme. Reasons were given to justify these choices but it might be worthwhile to explore other window types and other modulation schemes. Also, it would be beneficial to try the existing set-up on an even wider array of power amplifiers.

In the application presented here, the amplitude taper was used only as a means for spectral containment. However, it would be possible to use the LINC architecture to create amplitude effects for the purpose of modulation as well. There is a great deal of opportunity here that went unexplored.

7 References

[1] *Manual of Regulations and Procedures for Federal Radio Frequency Management*, NTIA, May 2011 Revision of January 2008 Edition.

[2] *ITU Manual of Radio Regulations*, No.119-08-Rev.1, 6 October 2008.

[3] H. Griffiths, S. Blunt, L. Cohen, and L. Savy, "Challenge problems in spectrum engineering and waveform diversity," *IEEE Radar Conference*, Ottawa, Canada, 29 Apr. – 3 May 2013.

[4] J. Jakabosky, S.D. Blunt, M.R. Cook, J. Stiles, and S.A. Seguin, "Transmitter-in-the-loop optimization of physical radar emissions," *IEEE Radar Conference*, Atlanta, GA, 7-11 May 2012.

[5] S.D. Blunt, M. Cook, J. Jakabosky, J. de Graaf, and E. Perrins, "Polyphase-coded FM (PCFM) radar waveforms, part I: implementation," accepted to *IEEE Trans. Aerospace & Electronic Systems*.

[6] S.D. Blunt, J. Jakabosky, M. Cook, J. Stiles, S. Seguin, and E.L. Mokole, "Polyphase-coded FM (PCFM) radar waveforms, part II: optimization," accepted to *IEEE Trans. Aerospace & Electronic Systems*.

[7] F.H. Raab, P. Asbeck, S. Cripps, P.B. Kenington, Z.B. Popovic, N. Pothecary, J.F. Sevic, and N.O. Sokal, "Power amplifiers and transmitters for RF and microwave," *IEEE Trans. Microwave Theory & Techniques*, vol. 50, no. 3, pp. 814-826, Mar. 2002.

[8] C. Baylis, M. Moldovan, L. Wang, and J. Martin, "LINC power amplifiers for reducing out-of-band spectral re-growth: a comparative study," *IEEE Wireless and Microwave Technology Conference*, Melbourne, FL, 12-13 Apr. 2010.

[9] N. Levanon, E. Mozeson, *Radar Signals*, Wiley – IEEE Press, 2004.